People's Democratic Republic of Algeria
Ministry of Higher Education and Scientific Research

University M'Hamed BOUGARA – Boumerdes

Institute of Electrical and Electronic Engineering

Department of Electronics

Final Year Project Report Presented in Partial Fulfilment of
the Requirements for the Degree of

MASTER

In **Telecommunication**

Option: **Telecommunications**

Title:

DESIGN AND ANALYSIS OF METAMATERIAL-INSPIRED MINIATURIZED DUAL-BAND ANTENNA

Presented by:

- **Aya GUERRACHE**
- **Rania CHALABI**

Supervisor:

Dr. K. DJAFRI

Registration Number: ..... /2023

Dedications

إلى:
السند الدائم صاحب السيرة العطرة والفِكر المُستنير، أبي لونيس. كُل دينٍ عليّ سوف أقضيه يوما إلا دينك فلن أقدِر عليهِ. جزاك الله عنّا خيرا...
من أي أبواب الثّناء عساي أدخُل وبأيّ أبيات القصيد أُعبّر. لعا تتبدى سيرتك وذِكرُ مناقبك وأفضالك، لا الكلمات تُعبّر ولا العبراتُ تفي بالغرض، ولو أنّي أوتيتُ كُلّ بلاغةٍ وأفنيتُ بُحور الشعر والنثر لكُنت بعد القول إلا مقصّرةً. كيف لا وأنت من اِتّخذت التضحية والعطاءِ عنوانا لأُمومتِها؛ حبيبة روحي وصاحبة دربي، أمي الجميلة حجاب خيرة. عسى الله أن يجزيك عني الفردوس...
توأمي، رفيقة طفولتي، شبابي وهَرمي باذن الله، فاطمة أختي الكبرى ومن فضلها عليّ أكبرُ. لا يسعني إلا أن أقول لولا وجودك في حياتي لكان انطبق عليّ قولُ الشاعر:

أخاك أخاك إنّ من لا أخ له كساعٍ إلى الهيجا بغير سلاح

ريحانات بيتنا وسِرٌ حيويته وبهجتهِ: مريم ونجمة، حفظكن الله من كلّ سوءٍ ولا أراني فيكن بأسًا...
سُكرة حياتي وأولى بناتي، من منحتني شعور الأمومة دون أن أكون أمًا. فلذة كبدي وأغصان ورق الجنة أفنان. أسأل الله أن يُنبتك نباتًا حسنًا وأن يجعلك ذخرًا للأمّة...
إلى من فرّق بيننا وبينه كأس العنون، جدي الغالي العيد، وددتُ لو انّك شاطرتني فرحتي. رحمك الله وأسكنك فسيح جنانه...
داعمي الاول والمؤمن بي وقدراتي ولو ولّى كل الناس ظهورهم لي، جدي عيسى، حفظك الله وختم لك بالخير..
وهل كان توفيقي ليكتمل دون دعواتكُن التي تحفني في غيبتي قبل حضرتي، جدتاي نجمة والزهرة، حفظكما الله ومدّ من عمريكما في طاعته...

حين ذكر العائلة فانّ عائلتي الصغيرة لا يسعُها الا أن تشمل عمّاتي وخالاتي وأولادهن، فلطالما كنتم جزءً لا يتجزّأ مِنّا...
لا قول عمّتي بل أقول أختي كريمة، أصدقُ العشاعرتلك التي أكنّها لك أنت وصغارك...
حيرتي لا تزال قائمة أأنزلك مقام أمي الثانية أم أختي،خالتي زهيرة، هبة الرحمن أنت واولادك...
كلُ الفتيات يقُلن أنّهن يعلن لصُحبة خالاتهن الأقرب منهن سنًا. أعذرهن حقا، فهنّ لا يعلُكنكُنّ في حياتهن، خالتاي فريدة وفاطمة، شكرًا على الدعم والحب الصادق...

الصداقة رزق وقد أوتيتُ من الأرزاق أفضلها،
مشاطرتي جُلّ ذكرياتي وراسمتها معي، ابتهال...
من آمنت بي ووقفت سدًا منيعًا ضدّ وهني، ايناس...
أميرتي الجميلة، مصدر الدعم وصاحبة أطيب قلب، اميرة...
شبيهتي وشطر روحي الثاني، ليديا، شكرا على كل شيئ وجزاك الله عني خيرا...
الى اللواتي قضيت معهن جُل أوقاتي هذه السنة، سيرين، شيماء و شيماء، شكرا فقد كنتن في طريق الشوك وردا يفوح شذاه عطرا...
مُرٌ عليّ بأن أودّع زائرا فكيف بمن حملتهم في أضلعي، أسأل الله أن يجمعنا في جنته كما جمعنا في الدنيا...

الأيام الصعاب تطوى ولا تطوى معها ذكرى من ساندنا فيها و مد لنا يد العون،
شكر خاص موصول للعائلة بلحاج، يسرتم عليّ يوم ضاقت، يسر الله لكم كل معسر...
الى من آزرني طوال هذه الفترة وهوّنها عليّ بكلمة طيّبة تارة وبدعوات كالبلسم تارة، جزاكم الله خيرا...
الى التي صبرت، تعبت، تحدت، ونهضت كُلّ مرّة بعد العثرات التي خالتها النهاية، الى نفسي،أحمد الله أن وهبك هذه التركيبة الفذّة المتناقضة، شكرًا لك وأمضي قدما...
الى كل من يقرأ...
أهدي هذا العمل المتواضع؛ أحبكم في الله...

To my beloved family, cherished friends, and invaluable supporters.

I dedicate my FYP to each and every one of you who have played an instrumental role in my journey.

Your unwavering love, guidance, and assistance have been the cornerstone of my success, and I am forever grateful for your presence in my life.

To my dear father, Abdelkader, and my loving mother, Ouahiba, your unconditional love, endless encouragement, and belief in my abilities have been my driving force. Your sacrifices and unwavering support have shaped me into the person I am today.

To my brothers, Hakim and Yacine, and my sister, Dounia, you have been my pillars of strength. Your constant encouragement, understanding, and shared laughter have made this journey more meaningful and enjoyable.

To my dear grandparents, with a special mention to my beloved grandmother, thank you, dear grandmother, for being an extraordinary role model, a source of unconditional love, and a guiding light in my life.

This achievement is a testament to your love and the values you have instilled in me.

To my nephew, Yasser, your innocent smile and boundless energy have brought immense joy to my life.

To my dear friend, Hamrioui Fatma Zohra, your unwavering support, invaluable insights, and

assistance throughout this project have been invaluable. Your dedication and belief in my abilities have meant the world to me.

To my project partner, Guerrache Aya, our collaboration and teamwork have been nothing short of extraordinary.

To my dear friends, Ikram, Sarah, and Hassina, thank you for your unwavering friendship, encouragement, and support.

This dedication is a small token of my deep appreciation and gratitude for each and every one of you.

Thank you for being my rock, my inspiration, and my cheerleaders. This achievement is as much yours as it is mine.

With heartfelt gratitude and love.

Rania

Acknowledgments

In the name of Allah, the most gracious and the most merciful, all praise to him for giving us the patience, the courage and the strength throughout this experience to complete this humble work successfully.

Alhamdulillah

Who does not thank people, is not thankful to ALLAH, it is our pleasure to thank those who made this report possible.

First and foremost, we express our sincerest gratitude to our supervisor Dr. K.DJAFRI her professional advices, guidance and time spent making things clear and simply was fundamental for the realization of this work.

Special words of thanks with gratitude are devoted to Pr. A. AZRAR and Pr. M. CHALLAL for their constant guidance and encouragement during our class as a telecommunication student.

Finally, we would like to thank our family members for all of their overall encouragement and provided support. Many thanks go as well to all institute's teachers who have contributed directly or indirectly to our five-year journey in the institute.

Abstract

This project introduces a design of a low-profile coplanar waveguide fed metamaterial-inspired dual-band microstrip antenna suitable for Wireless Local Area Network WLAN applications. The proposed antenna has a compact size of 18×20 mm², fabricated on an FR-4 substrate with a dielectric constant ε_r=4.3, and utilizes a double split ring resonator SRR triangular geometry to achieve dual-band operation. The antenna operates within two distinct frequency bands [*2.38-2.52GHz*] and [*4.24-8.1GHz*], covering the entire WLAN spectrum [*2.4-2.48GHz*], [*5.15-5.35GHz*], and [*5.725-5-825GHz*].

The prototype of the proposed design is fabricated and measured. A fairly good agreement was achieved between the simulated and measured frequency responses of the reflection coefficient indicating that the proposed metamaterial-inspired dual-band antenna is suitable for WLAN applications.

Finally, a comparative study is also presented to show the performance of the proposed antenna with respect to other conventional antenna structures in terms of overall size, bandwidth, and reflection coefficient. The findings highlight the antenna's competitive advantages, such as wide bandwidth and favorable reflection coefficient, while maintaining a compact size.

Table of Content

List of Figures

List of Tables

List of Abbreviations

2D	Two Dimensional
3D	Three Dimensional
AMC	Artificial Magnetic Conductor
CPW	Co-Planar Waveguide
CST	Computer Simulation Technology
dB	Decibels
dBi	Decibels by Isotropic
DNG	Double Negative
DPS	Double Positive
EBG	Electromagnetic Band Gap
ENG	Epsilon Negative
FSS	Frequency Selective Surface
GHz	Gega Hertz
HIS	High Impedance Surfaces
LHM	Left Hand Medium
LTE	Long Term Evolution
mm	Millimeter
MPA	Microstrip Patch Antenna
MNG	Mu Negative
NIM	Refractive Index Metamaterial
PEC	Perfect Electric Conductor
PMC	Perfect Magnetic Conductor
RHM	Right Hand Medium
SRR	Split Ring Resonator

VSWR Voltage Standing Wave Ratio

VNA Vector Network Analyzer

WLAN wireless local-area network

WiMAX Worldwide Interoperability for Microwave Access

List of Symbols

λ_0	Free space wavelength
ε	permittivity
ε_r	Relative permittivity
μ	Permeability
Γ	Reflection Coefficient
π	Pi number
D	Directivity
E	Electric Field
H	Magnitic Field
Pin	Input Power
$Prad$	Radiated Power
U	Radiation Intensity
$S11$	Input Reflection Coefficient
Zin	Input Impedance
Z_0	Characterestic Impedance

General Introduction

The Wireless Local Area Network WLAN has gained significant recognition as a highly convenient and straightforward connectivity solution worldwide. It offers several notable advantages, such as easy connectivity for high-speed data transmission, enhanced user mobility, and cost-effectiveness [1]. In the current era, where there is a high demand for simultaneous operation of numerous handheld electronic devices, the integration of dual-band antennas has become essential for wireless communication systems.

Traditional microstrip antennas have been developed to provide dual-band functionality. However, they face various challenges related to miniaturization, operating at multiple frequencies, enhancing bandwidth, gain, and efficiency [2]. To address these limitations, researchers have turned to artificially engineered structures known as metamaterials. These unique electromagnetic structures possess properties that are not naturally found in materials. By incorporating metamaterials into planar technology, the challenges faced by microstrip antennas can be overcome.

A major advantage of Metamaterial-Inspired antennas is their compact size relative to the operational frequency wavelength [3]. This characteristic makes them particularly suitable for applications like WLAN, Worldwide Interoperability for Microwave Access WiMAX, and other wideband applications. In addition to their utilization to achieve miniaturization to a certain extent, they can be used to enhance bandwidth and gain.

This project deals with the design, analysis, and fabrication of a miniaturized metamaterial inspired dual-band antenna. The proposed antenna performances in terms of operating bands, matching, bandwidth and radiation pattern are simulated and evaluated using CST software. This report includes three main chapters organized as follows:

- **Chapter one:** This chapter is divided into two main sections. The first section provides an overview of microstrip antennas, including their fundamental parameters. The second section briefly introduces metamaterials, covering their history, types, and advantages…

- **Chapter two:** This chapter focuses on the design of a slotted triangular ring antenna specifically for WLAN working bands. It presents a detailed procedure for achieving the final design and includes various parametric studies conducted to understand its operating mechanism. The chapter also discusses the results obtained from these studies.

- **Chapter three:** In this chapter, the triangular slotted ring antenna design presented in Chapter two is enhanced by incorporating metamaterial-inspired characteristics. This is achieved by adding an additional slotted ring inside the first ring. By integrating these metamaterial features and analyzing the obtained structure, it is concluded that the size of the antenna can be effectively reduced. Subsequently, a size reduction of about 25% is achieved as compared to the mono ring slotted antenna.

Furthermore, for experimental validation, the proposed antenna is fabricated and tested. A comparison between the simulated and measurement results is found to be in good agreement. This allows for an evaluation of the antenna's performance and validates the effectiveness of the metamaterial-inspired modifications.

Chapter One
Generalities on Microstrip Antennas and Metamaterials

Generalities on Microstrip Antennas and Metamaterials

1.1 Introduction

Microstrip antennas offer numerous benefits, making them widely used in various applications. They are known for their compact size, low profile, low cost and ease of integration. However, microstrip antennas also have certain drawbacks. These include narrow bandwidth, limited radiation efficiency, and restricted directivity control. Metamaterials, on the other hand, offer unique electromagnetic properties that can address these drawbacks by incorporating metamaterial structures into microstrip antennas, unlocking new possibilities for high-performance antenna designs.

1.2 Microstrip Antennas

Although they date back to 1953, microstrip antennas were first patented in 1955. The 1970s saw a rise in their development and use in aircraft, spacecraft, satellite, and missile applications, as well as mobile radio and wireless communications; this is due to the fact that they are naturally lightweight, inexpensive to produce, simple to install and they are characteristically low profile.

Microstrip antennas consist of very thin metallic patch printed on a grounded substrate with thickness h. Figure 1.1[4] shows a simple rectangular microstrip antenna.

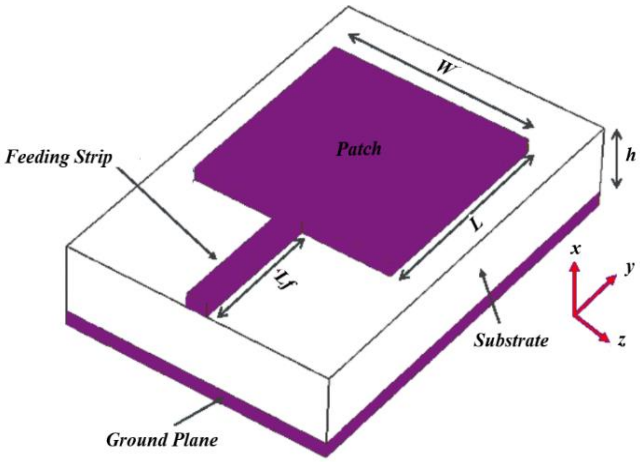

Figure 1.1 Rectangular MPA structure[4]

Several dielectric materials can be used for substrate in the antenna design. Their relative dielectric constants are generally in the range $2.2 \leq \varepsilon_r \leq 12$. The most suitable ones for good radiation performances are thick with lower relative permittivity because they ensure better radiation efficiency, larger bandwidth but at the expense of larger element size. Thin substrates with higher dielectric constant are desirable for microwave circuitry because they

need tightly bound fields to minimize unwanted radiation and coupling. However, they are considered less efficient and they have relatively narrow bandwidth due to their great losses [4] .

Different geometric shapes, including square, elliptical, triangular, rectangular, and circular (Figure 1.2) can be used to create patches. In order to meet the demands of a particular application, more intricate patterns based on regular shapes have been introduced.

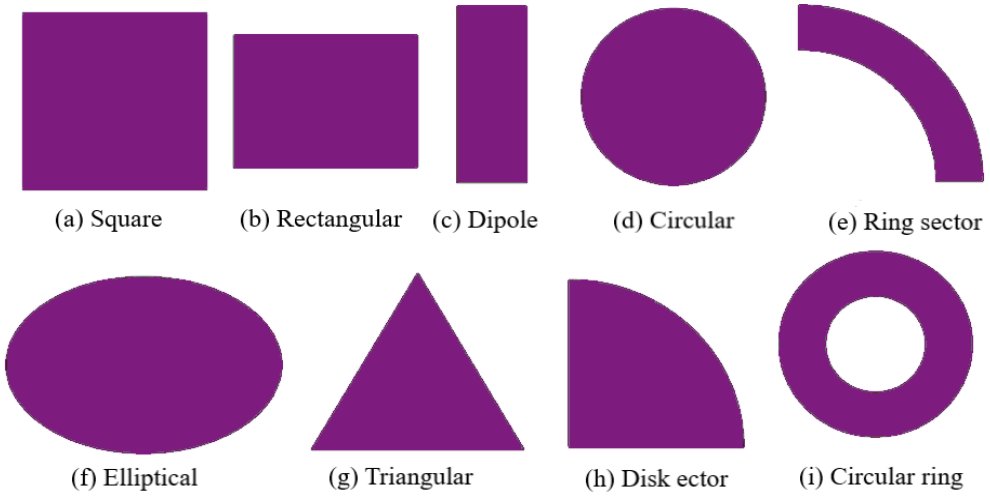

Figure 1.2 Representative shapes of Microstrip antenna

1.2.1 Microstrip Antenna Working Principle

As the patch must resonate at a specific frequency to efficiently radiate an electromagnetic wave; the cavity and fringing effects play an important role in the operation of microstrip patch antennas since they both have an impact on how these waves are resonated and radiated.

The cavity effect refers to the resonance that occurs within the patch itself. The patch and the surrounding air form a resonant cavity, which allows the antenna to resonate at a specific frequency, are determined by the dimensions of the patch and the dielectric constant of the substrate. This resonance causes the patch to act like a resonant circuit, which generates a standing wave pattern within the patch. On the other hand, the fringing effect refers to the way that the patch radiates electromagnetic waves. The fringing effect is due to the presence of electric field fringes that extend beyond the patch and into the surrounding air. These fringes are caused by the interaction between the patch and the transmission line that feeds the patch. The fringes cause the patch to radiate electromagnetic waves, which are then transmitted through the surrounding air.

1.2.2 Feeding Techniques

The design of the feeding structure directly affects the impedance matching, operating modes, spurious radiation, surface waves, and geometry of the antenna. The feeding structure thus plays a vital role in widening the impedance bandwidth and enhancing radiation performance [5].

There are numerous ways to feed microstrip patch antennas which are mainly categorized into two types: contacting and non-contacting, the flowchart in Figure 1.3 classifies these techniques. In the contacting approach, a connecting component is used to supply the RF power directly to the radiating patch. Electromagnetic field coupling is used in the non-contacting system to transfer power between the microstrip line and the radiating patch.

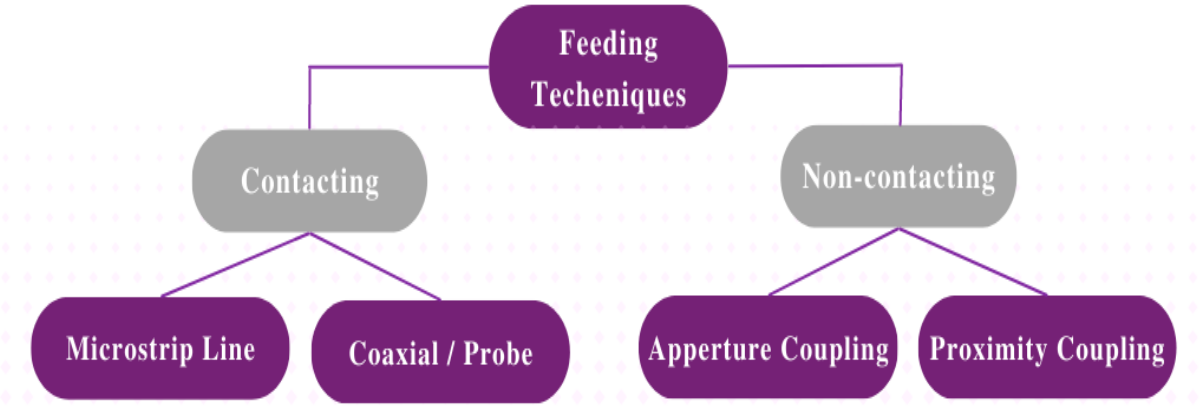

Figure 1.3 Feeding techniques categories

a. Coaxial Feed

The most popular method for feeding MPAs is the coaxial feed, often known as the probe feed. The coaxial connector's inner conductor extends through the dielectric and is attached to the radiating patch, as shown in Figure 1.4 (a), while the outside conductor is linked to the ground plane. The primary benefit of this feed arrangement is the flexibility with which the feed can be positioned inside the patch to best match the input impedance, it also has low spurious radiation and it is simple to manufacture. However, the fact that it was attached to the ground plane connector was a huge drawback.

b. Microstrip Line Feed

The microstrip line feed is a contacting feed technique where a conducting strip is attached directly to the microstrip patch's edge as shown in Figure 1.4 (b). Its advantage is

that the feed can be etched on the same substrate to give a planar structure, even though the conducting strip is narrower than the patch. Also, the matching can be achieved without any use of extra matching components, rather simple to fabricate and model.

c. Aperture Coupled Feed

In aperture coupling, the radiating microstrip patch element and the microstrip feed line are etched on the antenna substrate's top and bottom, respectively. In accordance with the dielectric constants ε_r and thickness, we select two distinct substrates. The lower one is constructed with high ε_r to limit spurious radiations, while the upper one is made with small ε_r to get better radiation. The amount of coupling from the feed line to the patch is determined by the form, size, and position of the aperture.

d. Proximity Coupled Feed

The electromagnetic coupling system is another name for this kind of feeding technique. It also has two dielectric substrates where the feed line lies, and the radiating patch is placed on top of the lower substrate. This feed approach has the advantages of eliminating spurious feed radiation and providing very high bandwidth (as high as 13%) [3].

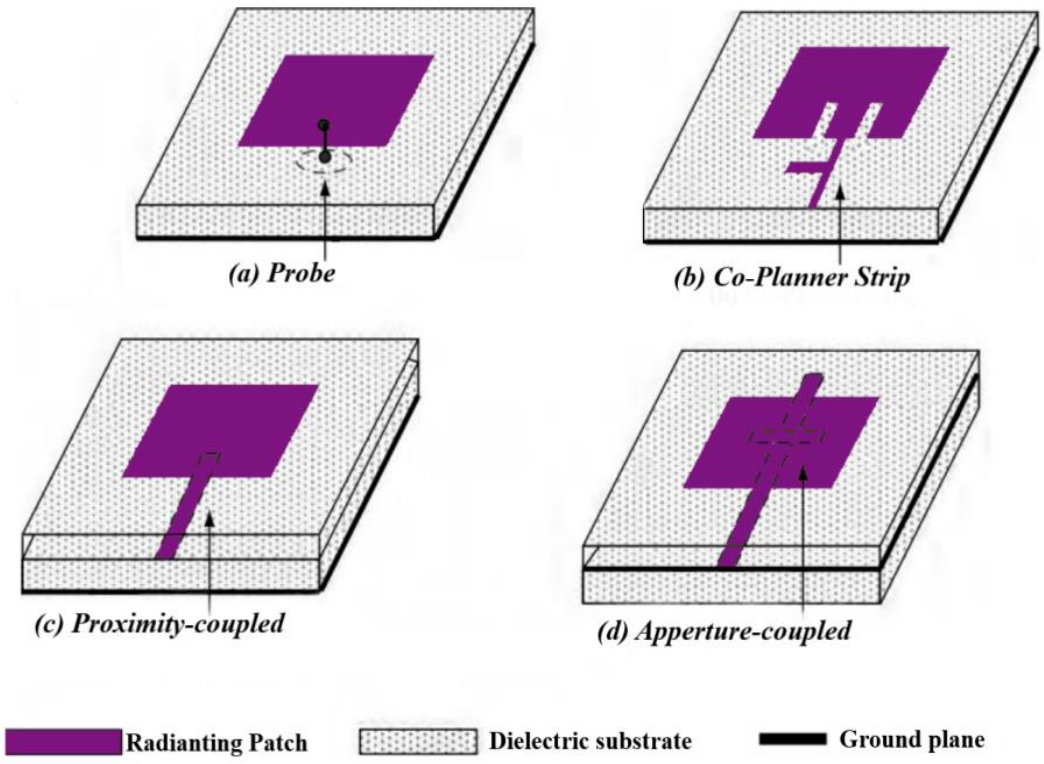

Figure 1.4 Typical feeds for microstrip antennas [4]

1.2.3 Methods of Analysis

A proper analysis of the microstrip antenna is crucial in order to optimize its performance in terms of gain, bandwidth, radiation efficiency, and impedance matching, among others.

There exist many methods of microstrip antenna analysis; the most popular are the transmission line model (in which we assume that the patch is a transmission line or a part of a transmission line), the cavity model (here we assume that the patch is a dielectric – loaded cavity), and the full wave (which include primarily integral equations and moment method). The three methods are summarized in the table 1.1 [7].

Table 1.1 Comparison between some analysis methods[7]

The method	Transmission Line	Cavity Model	Full wave
Accuracy	Less accurate	More accurate	Very accurate
Coupling Model	Hard	Hard	Easy
Difficulty	Easiest	Complex	Most complex
Physical insight	Good	Good	Bad

1.2.4 Basic Antenna Parameters

To fully characterize an antenna when designing it, a variety of parameters can be analyzed; some of them are outlined below.

a. Input Impedance

The input impedance is an important consideration to have better results of an antenna granted on a transmitter or a receiver. By definition, the input impedance of an antenna is the impedance presented by an antenna at its terminals or the ratio of the voltage-current at a pair of terminals. It is given by the following formula:

$$Z_{in} = Z_0 \frac{1+\Gamma}{1-\Gamma} \qquad 1\text{-}1$$

b. Impedance Bandwidth

The impedance bandwidth describes the bandwidth over which the antenna has acceptable losses due to mismatch. The impedance bandwidth can be measured by the characterization of both the voltage standing wave ratio *VSWR* and return loss *RL* at the frequency band of interest. Both *VSWR* and *RL* are dependent on measuring the reflection coefficient Γ at the terminals of the antenna that is defined by [8]:

$$\Gamma = \frac{Z_{in} - Z_0}{Z_{in} + Z_0} \qquad 1\text{-}2$$

The *VSWR* is defined as the ratio between the voltage maximum and voltage minimum of the standing wave created by the mismatch at the load on a transmission line. The *VSWR* equation is shown in Equation 1-3 [8].

$$VSWR = \frac{1 + |\Gamma|}{1 - |\Gamma|} \qquad 1\text{-}3$$

The RL is the magnitude of the ratio of the reflected wave to that of the incident wave, and is defined in *dB* as [8]:

$$RL = -20\log\ |\Gamma| \qquad 1\text{-}4$$

c. Radiation Pattern

According to the definition, an antenna radiation pattern is "a mathematical function or graphical description of antenna features as a function of space coordinates." The directional coordinates are a function of the radiation pattern, which is defined in the far-field region. A polar graph is a 2-D or 3-D energy distribution that represents a radiation pattern, as showen in figure 1.5 . Most of the time, this radiation pattern is normalized and expressed in decibels *dB* [6].

The performance of the antenna is often described in terms of its principal E- and H-plane patterns [7].

- The E-plane pattern It is defined as the plane containing the electric field vector and the direction of maximum radiation.
- The H-plane pattern It is defined as the plane containing the magnetic field vector and the direction of maximum radiation.

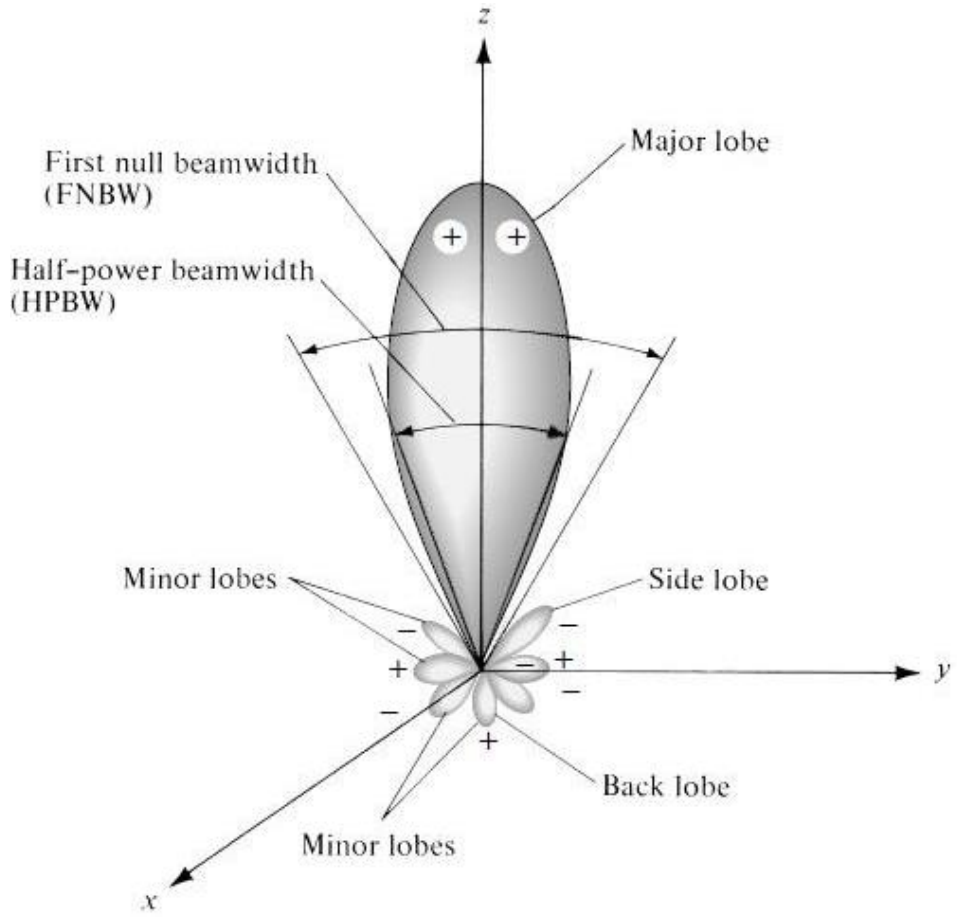

Figure 1.5 Radiation Lobes and Beam widths of the radiation pattern [6]

d. Beamwidth

The beamwidth is defined as the angular separation between two identical points on opposite side of the pattern maximum. Mainly two types of beamwidths exist which are:

- Half Power Beam Width HPBW is defined by IEEE as: "in a plane containing the direction of the maximum of a beam, the angle between the two directions in which the radiation intensity is one-half the maximum value of the beam" [8].
- First Null Beam Width FNBW is defined as the angular separation between the first null of the radiation pattern.

e. Polarization

The polarization of an antenna in a given direction is defined as the polarization of the radiated wave by the antenna. It is the time-varying direction and relative magnitude of the electric field vector. It is simply the orientation of the electric field component. There exist three types of polarization which are; Linear, Circular, and Elliptical, as shown in the Figure 1.6 [9].

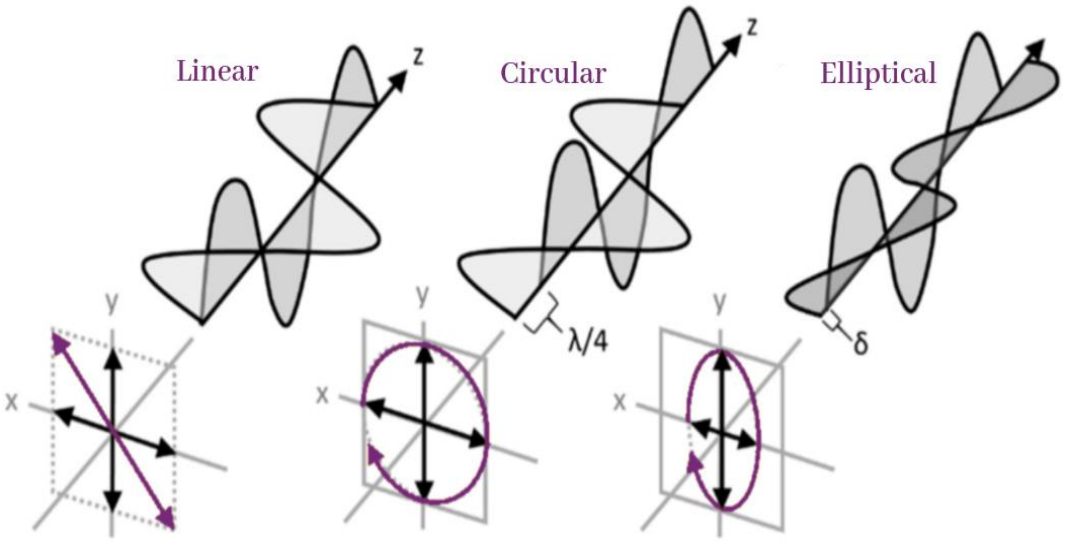

Figure 1.6 Linear, Circular and Elliptical polarizations

f. Directivity

The directivity of an antenna, *D*, is the ratio of the radiated power density to the radiated power density averaged in all directions [10]. The directivity is expressed in *dB* and is given by:

$$D = \frac{U}{U_0} = \frac{4\pi U}{P_{rad}} \qquad 1\text{-}5$$

Where:

U: radiation intensity (W/unit solid angle).

U_0: radiation intensity of an isotropic source (W/unit solid angle).

P_{rad}: total radiated power (W)

g. Gain and Efficiency

Another useful measure describing the performance of an antenna is the gain. Although the gain of the antenna is closely related to the directivity, it is a measure that takes into account the efficiency of the antenna as well as its directional capabilities. It is defined as the ratio of the intensity, in a given direction, to the radiation intensity that would be obtained if the power accepted by the antenna were radiated isotropically. The radiation intensity corresponding to the isotropically radiated power is equal to the power accepted (input) by the antenna divided by 4π [11].

$$G = 4\pi \frac{\text{radiation intensity}}{\text{total input power}} = \frac{4\pi U}{P_{in}} \quad 1\text{-}6$$

Antenna efficiency is defined as the ratio of radiated power over input power; it is often given as a percentage, a decimal, or in *dB*, but is just a ratio with a value between zero and one.

$$\eta = \frac{P_{rad}}{P_{in}} \quad 1\text{-}7$$

1.3 Metamaterials

Metamaterials were first synthesized in 1968 by Veselago, who theorized that materials with negative permeability and permittivity could exist. In 1999, Pendry developed a practical technique for creating Left-Handed Materials *LHM* that do not follow traditional rules. In 2002, Lucent Technologies made a significant contribution to the field of metamaterials by using them to produce resonant antennas [12].

Metamaterials are artificially engineered materials that have unique electromagnetic properties that are difficult or impossible to achieve with conventional, naturally occur ring materials. The advent of metamaterial has yielded new opportunities to realize physical phenomena that were previously only theoretical exercise [13].

1.3.1 Properties of Metamaterials

The electromagnetic property of these metamaterials can be described by the Maxwell's equations. The transformation of this equation serves to highlight the properties of metamaterials. They are given in the set of equations:

$$\vec{\nabla} \times \vec{E} = -j\omega\mu\vec{H} \quad 1\text{-}8$$

$$\vec{\nabla} \times \vec{H} = j\omega\varepsilon\vec{E} \quad 1\text{-}9$$

Where $\vec{E}$ and $\vec{H}$ are the vectors of electric and magnetic fields strengths, respectively; ε and μ are the material permittivity and permeability; ω is an angular frequency; and $j=\sqrt{-1}$ is an imaginary number.

In the case of the plane wave propagation, the electric and magnetic fields are giving by equations 1-10 and 1-11 respectively; where $\vec{k}$ represents the propagation vector.

$$\vec{E} = \overrightarrow{E_0} e^{(-j\vec{k}.\hat{r}+j\omega t)} \quad 1\text{-}10$$

$$\vec{H} = \overrightarrow{H_0} e^{(-j\vec{k}.\hat{r}+j\omega t)} \quad 1\text{-}11$$

Where $\overrightarrow{E_0}$ and $\overrightarrow{H_0}$ are vectors in arbitrary directions. $\vec{k}$ a wave vector, r is the observation position vector.

In addition, to evaluate the properties of materials, a general definition of the Poynting power density vector $\vec{S}$ is mentioned, which is subdivided into the time $e^{+j\omega t}$ and the space e^{-jkr} components. The real part of the Poynting vector $\vec{S}$, which determines the energy flow, is represented by the following formula:

$$\vec{S} = \frac{1}{2} \vec{E} \times \vec{H}^* \quad 1\text{-}12$$

For the plane wave, the electric field $\vec{E}$ and the magnetic field $\overrightarrow{H}$ are defined by

$$\vec{k} \times \vec{E} = \omega\mu\vec{H} \quad 1\text{-}13$$

$$\vec{k} \times \vec{H} = -\omega\varepsilon\vec{E} \quad 1\text{-}14$$

In the isotropic and homogeneous medium, the values of ε and μ are simultaneously positive. In this medium, the electric field $\vec{E}$, magnetic field $\vec{H}$, and propagation vector $\vec{k}$ form the right circulate triad of orthogonal vectors. Therefore, it is also defined as the right-handed medium RHM, where the $\vec{S}$, $\vec{k}$ have the same directions and electromagnetic waves can propagate in them.

In that case, the values of Ɛ and μ are negative simultaneously; so, Equations 1-13 and 1-14 can be rewritten as:

$$\vec{k} \times \vec{E} = -\omega|\mu|\vec{H} \quad 1\text{-}15$$

$$\vec{k} \times \vec{H} = \omega|\varepsilon|\vec{E} \quad 1\text{-}16$$

In this case, the electric field $\vec{E}$, the magnetic field $\vec{H}$, and the propagation vector $\vec{k}$ form left-hand circulate triad of orthogonal vectors, which also is defined as the left-hand medium

LHM. In this medium, the poynting vector $\vec{S}$ has the opposite direction to the propagation vector $\vec{k}$; this is illustrated in Figure 1.7;so that it can support backward waves, i.e., the energy and wave fronts travel in opposite directions [14].

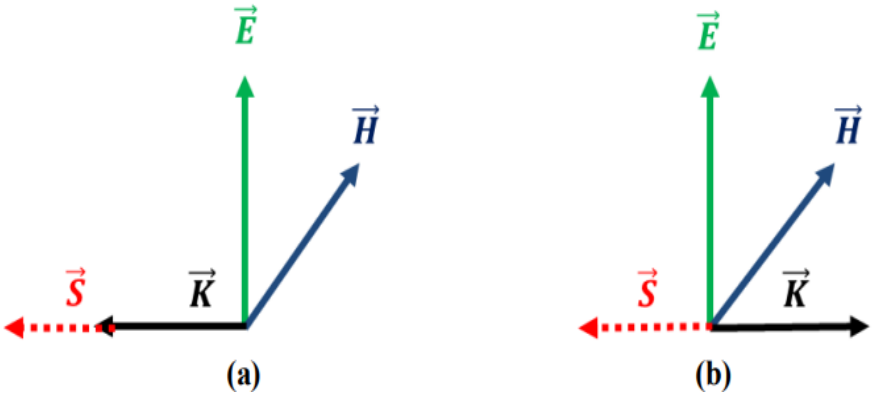

Figure 1.7 (a) Right-handed system, (b) Lefthanded system[14]

1.3.2 Metamaterials Classification

The response of a system to the presence of Electromagnetic field is determined by the properties of the materials involved. These properties are described by defining the macroscopic parameters permittivity and permeability of these materials. On the basis of its sign, the metamaterials can be classified into four groups as shown in Figure 1.8 .

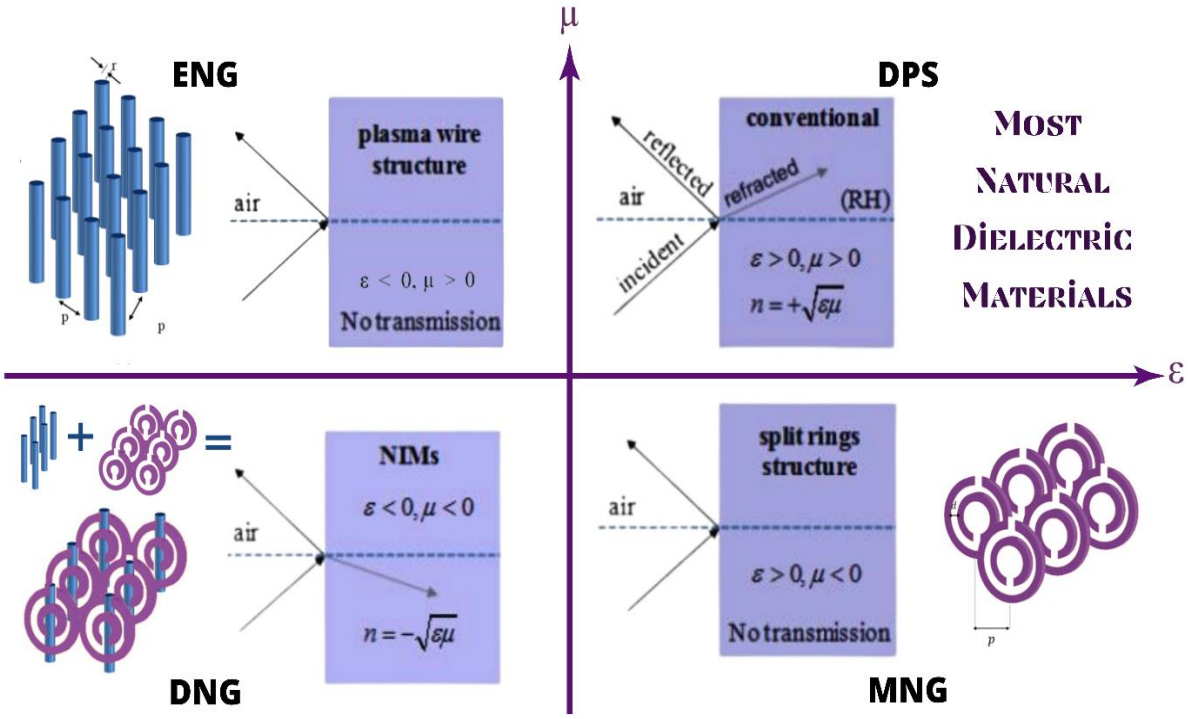

Figure 1.8 The classification of Metamaterials

a. Double Positive DPS Medium

A medium with both permittivity and permeability greater than zero ($\varepsilon > 0$, $\mu > 0$) is called as double positive DPS medium. They have the same properties as the Right-Handed Materials RHMs which are present in nature, such as in naturally occurring dielectrics permeability, resulting in wave propagation that travels in the forward direction [18].

b. Epsilon negative ENG Medium

A medium with ($\varepsilon < 0$, $\mu > 0$) is called as Epsilon negative ENG medium. Thin metallic wires are one of the most basic structures that produce negative permittivity at a certain frequency band. This The structure consists of infinitely long parallel thin wires of metal which have same radius *r* and are separated by a distance *p* from each other (see Figure 1.8) [16].

c. Mu negative MNG Medium

A medium with ($\varepsilon > 0$, $\mu < 0$) is called as mu negative MNG medium. It is the most popular structure has been using is split ring resonators SRRs. A unit cell of the SRR is composed of two concentric metallic rings and separated by a gap p. Each ring has a narrow slot, and they are generally spaced 180 degrees apart on each side. The gap between inner and outer ring acts as a capacitor, while the rings themselves act as an inductor. Therefore, the combination of the two rings acts as an LC resonance circuit [20].

d. Negative DNG Medium

A medium with ($\varepsilon < 0$, $\mu < 0$) is called as Double negative DNG medium. The combination of alternating layers of thin metallic wires and circular split rings, exhibits negative index of refraction resulting in backward wave propagation. Thus, it is referred to as NIM or negative index material. It is also called left-handed materials [19].

1.3.3 Types of Metamaterials

Electromagnetic metamaterials are a specialized class of materials that enable advanced control and manipulation of electromagnetic radiation.

a. Electromagnetic Bandgap EBG Metamaterials

Electromagnetic bandgap structures are known as EGB structures. They are also known as photonic bandgap structures PBG [18]. They are defined as artificial periodic structures

that avert or assist the propagation of electromagnetic waves in a specified band of frequencies for all incident angles and all polarization states. They are usually used as a component of microwave devices in order to improve the performance of devices specially to improve the radiation/gain patterns and to decrease the noise/losses in transmissions. EBG structures are also known as high-impedance surface due to their ability to suppress the surface wave at certain operational frequencis [19]. Figure 1.9 shows the EBG structure.

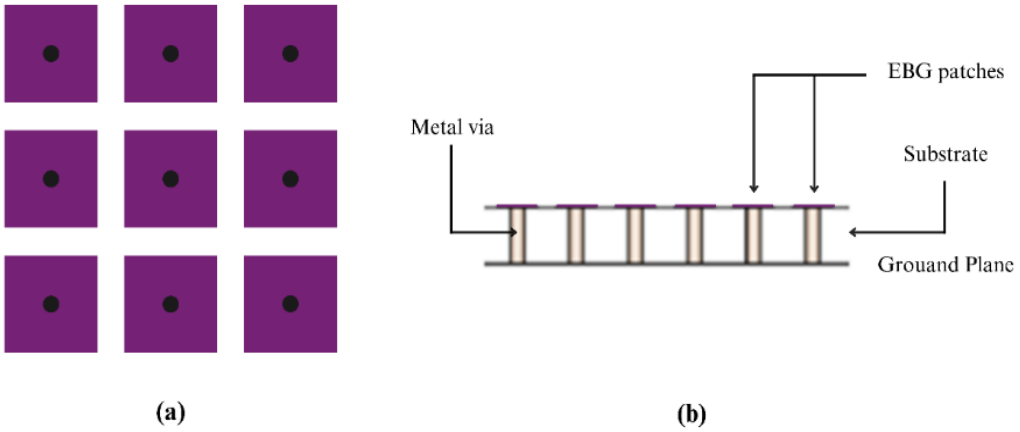

Figure 1.9 EBG structure (a) Top view, (b) Side view

b. Frequency-Selective Surface-based materials FSS

Frequency selective surfaces FSSs are made up of metallic patches arranged periodically, with various geometric shapes, or their complementary counterparts, which consist of aperture elements similar to the patches as can be seen in Figure 1.10. These surfaces demonstrate complete reflection or transmission in the vicinity of the resonant frequencies of the individual elements [20].

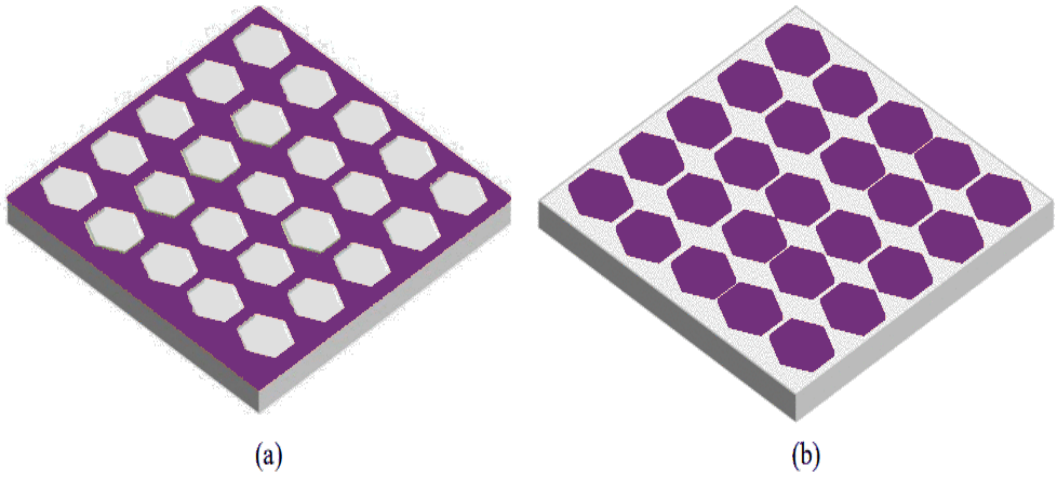

Figure 1.10 Two examples of metallic FSS

(a) Slot array on a dielectric sheet, (b) Dipole array on a dielectric sheet

c. Artificial Magnetic Conductor AMC

An AMC, or Artificial Magnetic Conductor, is a type of metamaterial that mimics the properties of a Perfect Magnetic Conductor PMC. It can provide zero-degree reflection phases at its resonant frequency, similar to a PMC. The AMC is also referred to as a High Impedance Surface HIS because it exhibits high surface impedance at its resonant frequency. The bandwidth of the AMC is defined as the range of frequencies where the reflection phase is within 0 ± 90° [16].

When an antenna is placed close to a metallic ground plane, such as a Perfect Electric Conductor PEC (see Figure 1.11 (a)), with a spacing less than λ/4, the 180° reflection phase causes destructive interference, resulting in poor return loss and low total efficiency. However, using an AMC as a ground plane (case (b) in Figure 1.11) can redirect the back radiation and provide shielding to the antennas, improving performance [16].

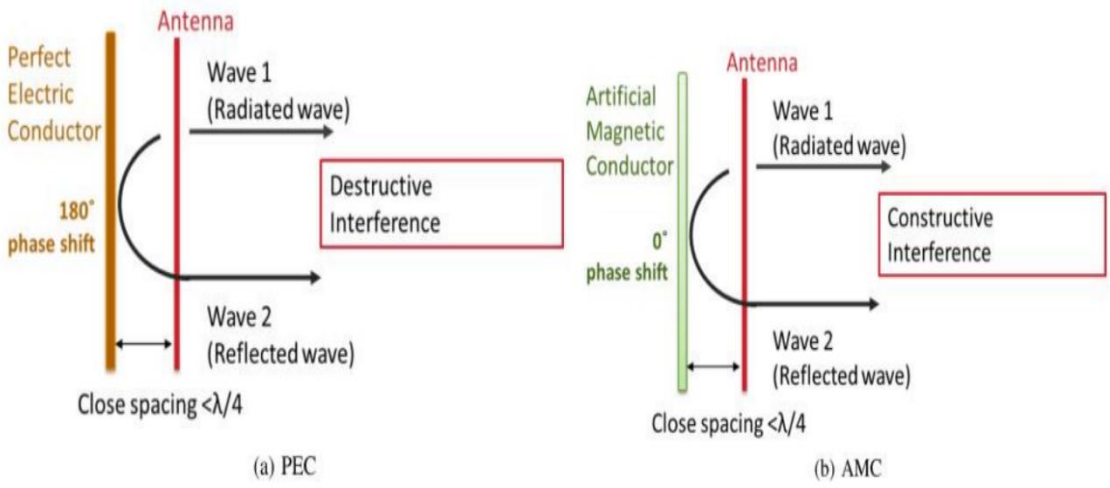

Figure 1.11 A radiator lying flat against, (a) PEC, (b) a Metamaterial AMC [16]

1.3.4 Applications of Metamaterials on Antennas

The field of metamaterials is rapidly evolving and ongoing research is expanding their potential in various areas of science, engineering, and technology. Figure 1.12 shows these main applications. One of their prominent uses is in antenna, where they can be used for:

- **Bandwidth Enhancement**: The demand for wideband antennas in modern wireless communication is rising, prompting the need for miniaturization and multiband capabilities. To address the narrow bandwidths of conventional patch antennas (typically 2% to 5%), various techniques have been employed. However, these techniques often introduce complexity and increase the antenna's size. Metamaterials provide a promising solution by

reducing complexity, eliminating the need for extra structures, and improving antenna performance.

- **Gain Enhancement:** Metamaterial antennas strategically incorporate metamaterial units to address lower gain in antennas. By placing them as loads on/near the patch, in the ground plane, within the substrate, or as a superstrate, these antennas enhance performance across various communication bands, improving gain and expanding the antenna's capabilities for optimal wireless communication.

- **Size miniaturization:** A recent approach involves utilizing metamaterials as a defected ground structure DGS to reduce antenna size. Metamaterials have unique properties at the antenna's resonance frequency, matching the dimensions of the removed parts of the DGS. This enables effective miniaturization of antennas [22].

- **Isolation:** Metamaterials enhance antenna isolation by strategically incorporating structures like resonators or reflectors near the antenna elements. These structures take advantage of their band gap characteristics, acting as effective notch filters to disrupt mutual coupling between neighboring antenna elements. This improves the overall isolation performance, reducing unwanted electromagnetic interference from nearby sources.

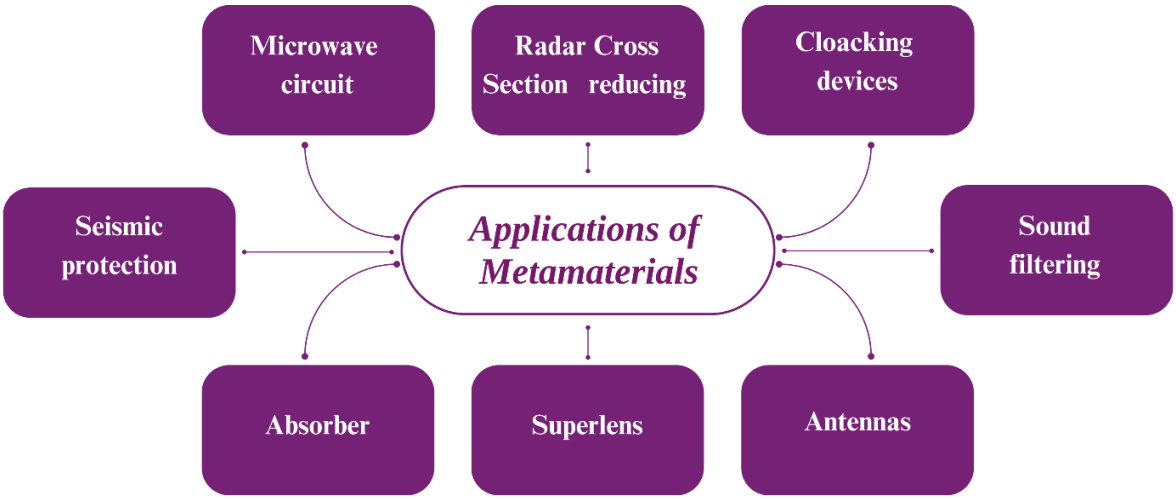

Figure 1.12 Main application of Metamaterials

1.4 Conclusion

This chapter is divided into two main sections. The first section provides a brief introduction to microstrip antennas, covering standard definitions, fundamental parameters, and characteristics. The second section introduces the concept of metamaterials, briefly discussing their properties, classification, types and main applications especially on antennas.

Chapter Two
Design of Dual Band Triangular Slotted Ring Antenna

Design of Dual Band Triangular Slotted Ring Antenna

2.1 Introduction

In modern wireless communication systems, various applications such as WLAN, WiMAX, Long Term Evolution LTE, and more operate on different frequency bands. Therefore, the significance of multiband operation, which can be achieved through the utilization of planar microstrip technology, becomes increasingly apparent. This technology enables a single antenna to radiate in different frequency bands at the same time, enhancing the overall performance of these wireless communication systems. In this chapter, a dual-band triangular ring antenna that covers WLAN *2.4GHz* and *5GHz* bands is presented. The design and simulation procedures are carried out using CST microwave studio MWS 2021.

The design procedure and evolution stages are investigated throughout the chapter, parametric analysis has been performed to improve the structure's operating characteristics.

2.2 Design Steps and Simulation Results

The use of triangular structures offers advantages such as compact size and convenient side-by-side coupling [21]. The triangular shape allows for more efficient utilization of space, making it suitable for applications where size constraints are a concern. Additionally, the triangular geometry facilitates easy coupling of multiple antennas placed alongside each other. However, they may have drawbacks such as narrow bandwidth, radiation pattern limitations, increased design complexity, sensitivity to surrounding objects, and challenges in impedance matching. For better understanding for this geometry, a study was conducted to investigate the impact of various parameters on it. During the study, each parameter was individually examined while keeping the other parameters constant, allowing for a focused analysis of their effects on antenna performance.

The proposed antenna is designed using an FR-4 dielectric substrate with relative dielectric permittivity ε_r= 4.3, loss tangent $tan\delta$ = 0.025 and thickness h=1.6 *mm*. It has a size of only 20 *mm* × 24 *mm*. We employ 50-Ω CPW to feed the antenna and square shaped ground plane.

The following sections provide a step-by-step procedure, beginning with a complete patch, leading to the final structure of a triangular slotted ring antenna.

2.2.1 Triangular Patch Antenna

The initial geometric configuration we started with in this work was a fully triangular-shaped patch antenna named 'Antenna I ' with equilateral legs denoted as *l2= mm* and a base length referred to as *l1= mm*. Different parametric studies have been done to each length to select the appropriate one. The input reflection coefficient S11 of this structure as well as its schematic are illustrated in Figure 2.2.

From the obtained S11 graph, it is evident that the triangular patch under consideration functions as a single operating band antenna, exhibiting a significantly wide band ranging from *3.2GHz* to more than *7 GHz*. Notably, the antenna demonstrates two resonances at *4.057 GHz and 5.086 GHz* with a remarkable reflection coefficient of *-29.44dB* and *-31.14dB*, respectively. This structure provides sufficient coverage for the second band, but it does not extend to cover the first band.

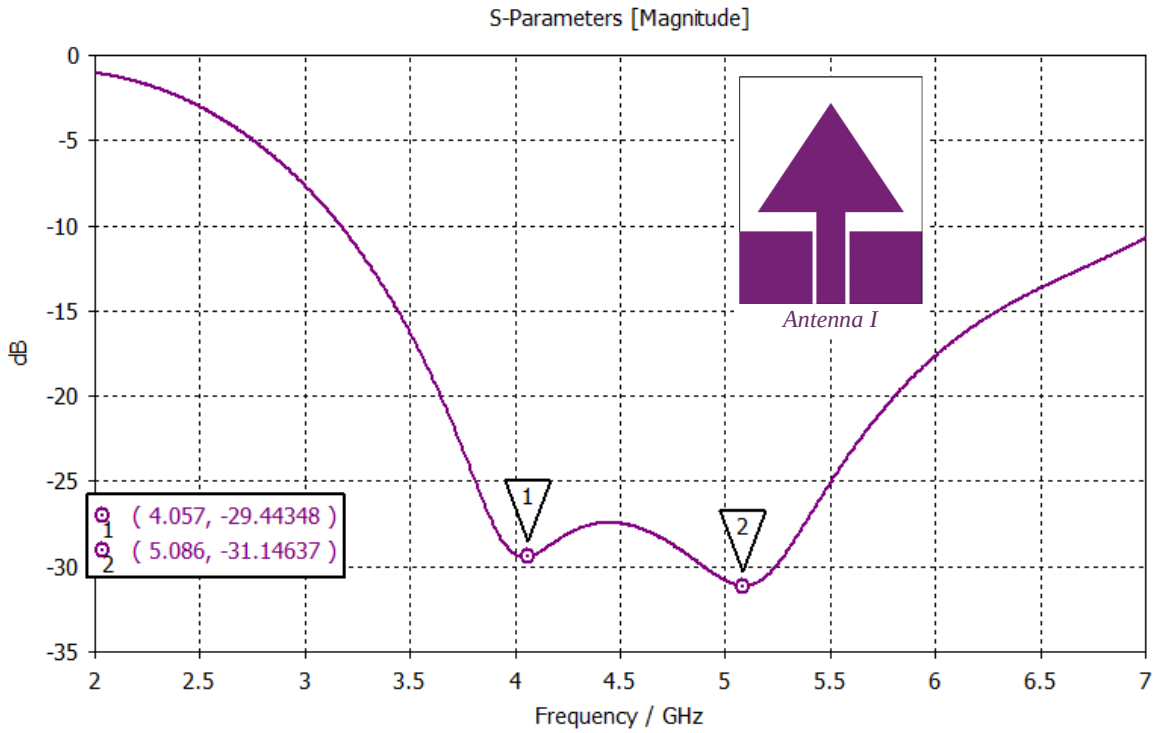

Figure 2.1 The Input Reflection Coefficient for the full patch -Antenna I-

a. Effect of varying the gap *d* between the patch and the ground

One of the parameters that have a significant effect on the antenna's operation is the gap *d* between the patch and the ground. A parametric study of this length has been done.

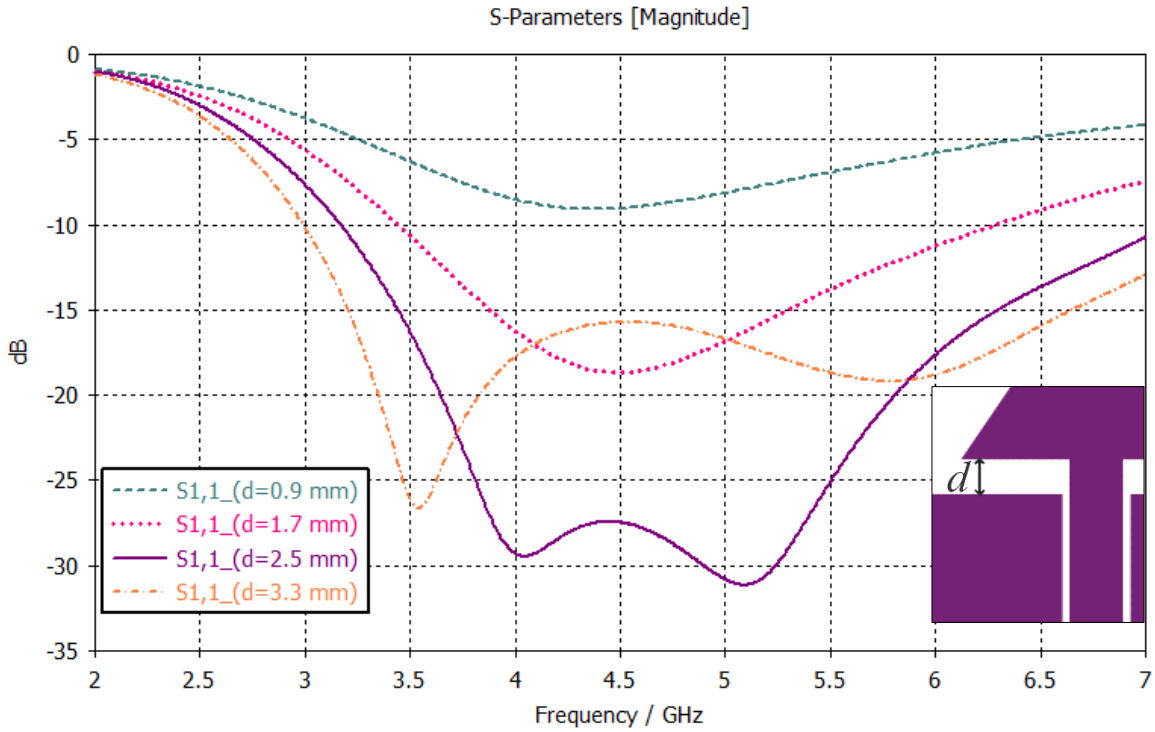

Figure 2.2 The effect of varying the gap d between the patch and ground on the S11

From the Figure 2.3 that shows the S11 plots for different values of *d*, it is noticed that when this gap is small (around 0.9 *mm*), the antenna fails to operate effectively. However, as the gap's length increases, the antenna begins to function and exhibits improved impedance matching. Looking across the whole spectrum, it is clear that the value *d*=2.5 *mm* provides optimal performance and the best matching. Therefore, it is recommended to maintain this length to avoid unnecessarily increasing the size of the antenna.

However, since the objective is to develop a dual band antenna, the subsequent proposed step involves introducing a triangular slot; transiting from the current patch antenna configuration to a ring antenna.

2.2.2 Triangular Ring Antenna

The introduction of a slot to transform a triangular patch antenna into a ring triangular structure can have significant effects on the S11 results, including alterations in the resonant frequency, bandwidth, radiation pattern and impedance matching. Additionally, this modification has the potential to facilitate the antenna's operation in multiple frequency bands. In our structure, it is observed that a new band emerges around *6.5GHz*, where the ring width value is *1mm* , indicating the successful achievement of dual-band functionality.

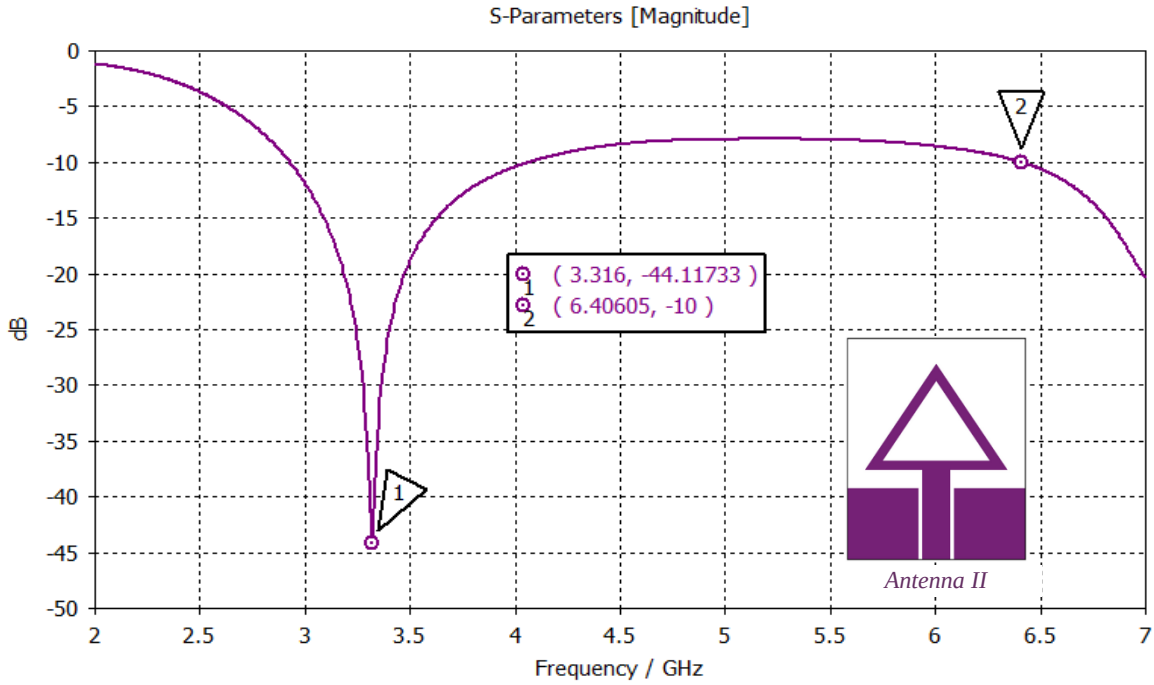

Figure 2.3 The Input Reflection Coefficient for the ring with width t -Antenna II-

a. Effect of varying the width of the ring *t*

The width *t* of the triangular ring may fall within the range of a few millimeters to a few centimeters. Its optimum value for our design specifications have been determined through simulations and optimizations. Figure 2.5 illustrates the parametric study results for this variable t.

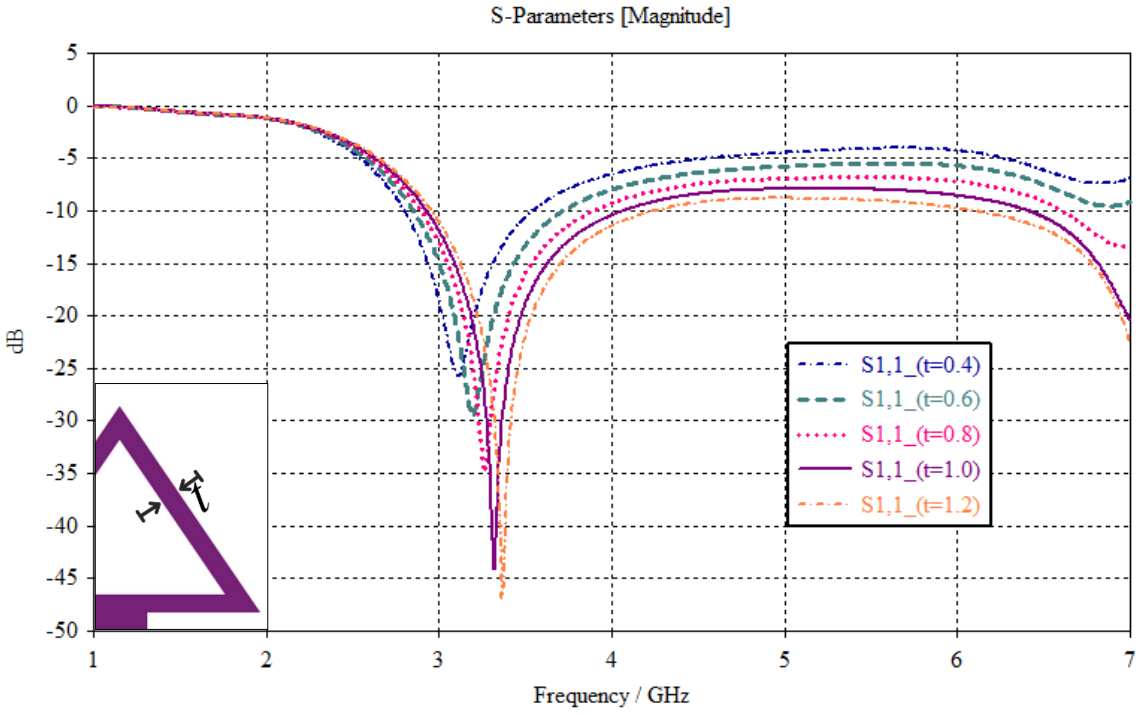

Figure 2.4 The effect of varying the ring's width on the input reflection coefficient

It can be observed that as the ring width *t* increases, a second band emerges, enabling dual-band operation. Simultaneously, the resonance frequency of the first band shifts towards higher frequencies and exhibits improved impedance matching. Furthermore, the second band experiences a shift towards lower frequencies. Consequently, the proximity of the two bands results in reduced isolation between them. To satisfy both requirements of dual-band functionality and an antenna operating at lower frequencies, we have opted for option *t* =1.

2.2.3 Slotted Triangular Ring Antenna

In order to address the challenge of achieving the desired frequency bands *2.4GHz* and *5GHz* for WLAN applications, modifications have been made to the previous structure. One approach involves incorporating a rectangular slot with a width of *ts* and a length of *t* into the leg of the triangular ring.

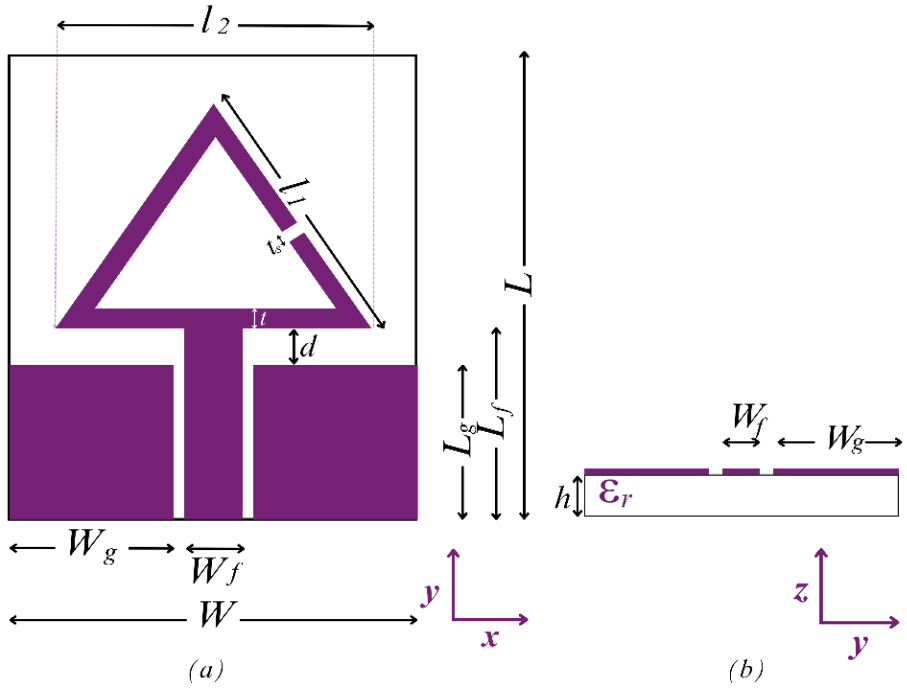

Figure 2.5 Schematic of the proposed Slotted Triangular Ring Antenna (a) Front view (b)Bottom view

Table 2.1 displays the dimensions of the proposed antenna including the length and width of the feed line and the rectangular ground dimensions that have been chosen so that the line impedance is 50 Ω.

Table 2.1 The dimensions of the triangular ring antenna

Parameter	*L*	*W*	*Lf*	*Wf*	*Lg*	*Wg*	*l1*	*l2*	*d*	*t*	*ts*
Value (*mm*)	*24*	*20*	*10*	*3.1*	*7.5*	*8.08*	*16*	*14*	*2.5*	*1*	*0.4*

Figure 2.6 depicts stepwise procedure to achieve the proposed antenna structure -Antenna III-, as well as the simulated S11 for the three steps, demonstrating a notable dual-band functionality when introducing the slot . The first band exhibits good matching, reaching *-27.94dB* at a frequency of *2.44GHz*. Furthermore, the simulated bandwidth with a reflection coefficient below -10 dB spans a narrow frequency range from *2.36GHz* to *2.52GHz*, aligning well with the requirements of WLAN applications. Moving to the second band, it initiates at *3.36GHz* and extends up to *7.4GHz*, with a resonance occurring at *4.44GHz* and a matching level of *-19.98dB*.

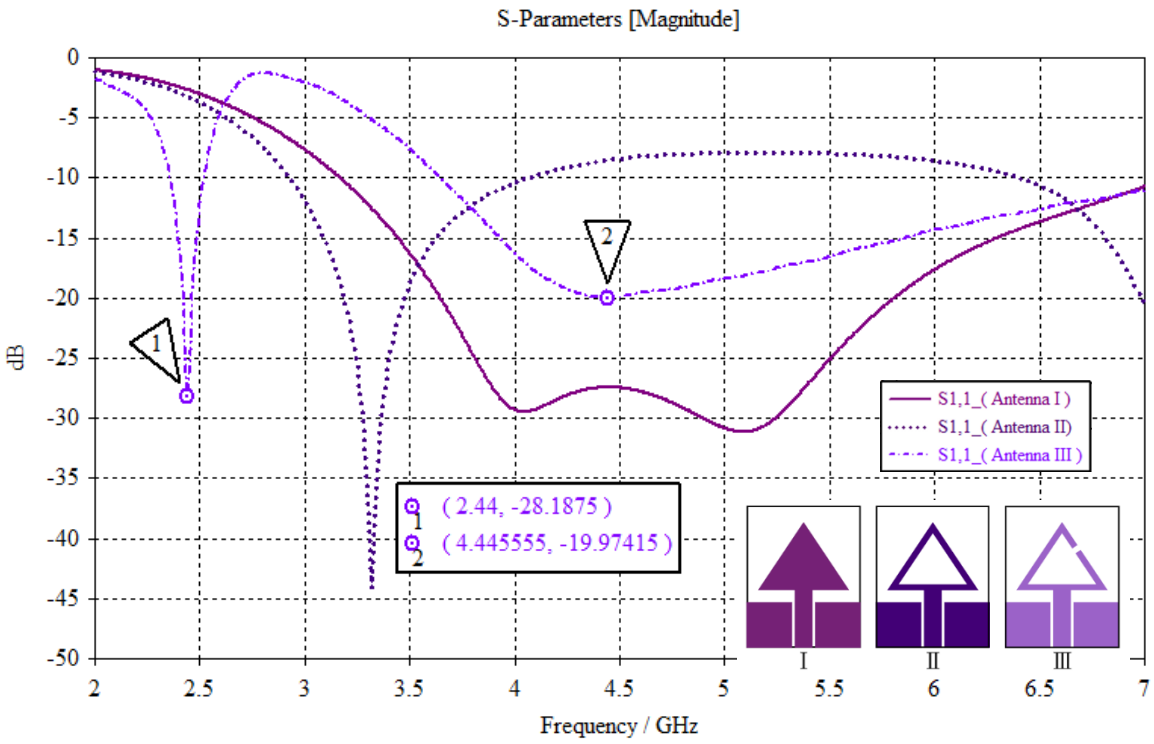

Figure 2.6 Stepwise procedure to obtain the desired frequency bands

The observed results highlight the capability of the proposed design to effectively operate in the specific WLAN applications dual frequency bands.

For a better understanding of the slot role, a parametric study of both position and length have been done, noting that when one parameter is considered the others are kept constant.

a. Effect of varying the slot width *ts*

The triangular slotted ring antenna works at low frequencies when the width of the slot is getting lower. The impact of the variation of the slot's width in the better reflection coefficient of $-26.62dB$ and appropriate first working band is shown in figure below.

The parameter *ts* mainly affects both working bands, while its impact on impedance matching is relatively minor. A narrower slot width causes a shift towards lower frequencies. This characteristic is especially crucial for the first band because we could achieve the applications requiring precise small frequency range.

Due to the specified design limitations, the simulations were halted when the slot width reached a minimum value of *ts=0.4mm*, which was subsequently adopted for further analysis.

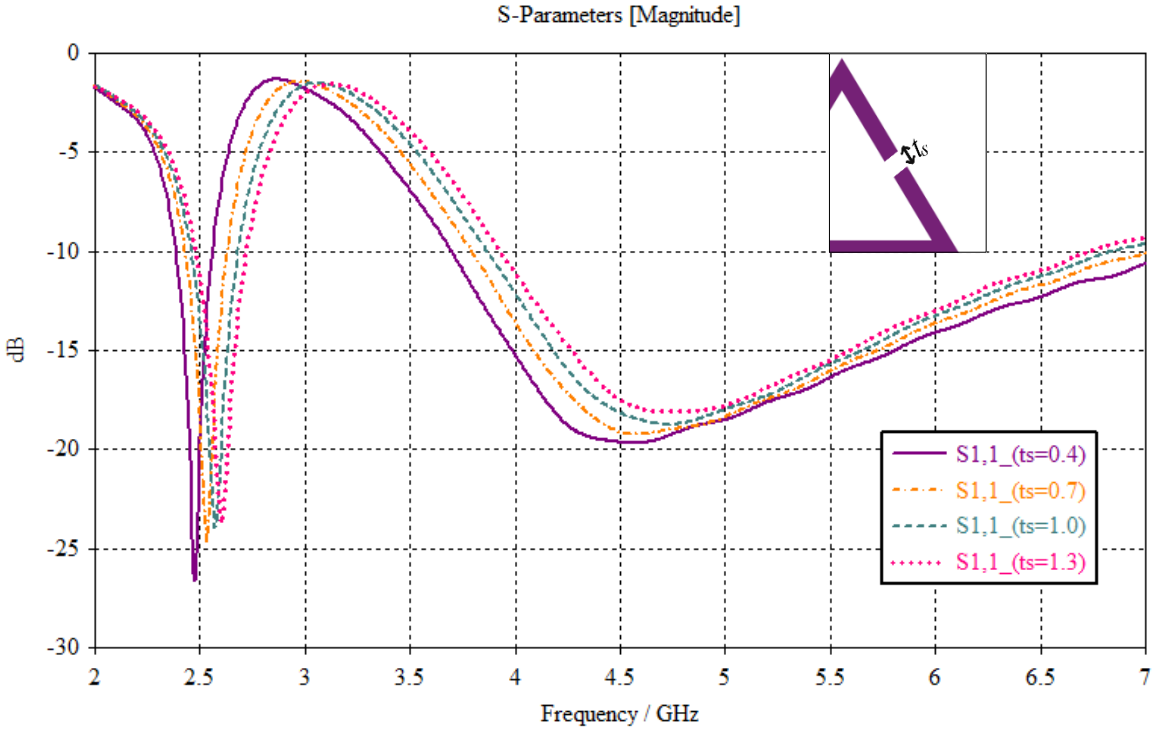

Figure 2.7 The effect of varying the width of the slot on the input reflection coefficient

b. Effect of varying the slot position *x*

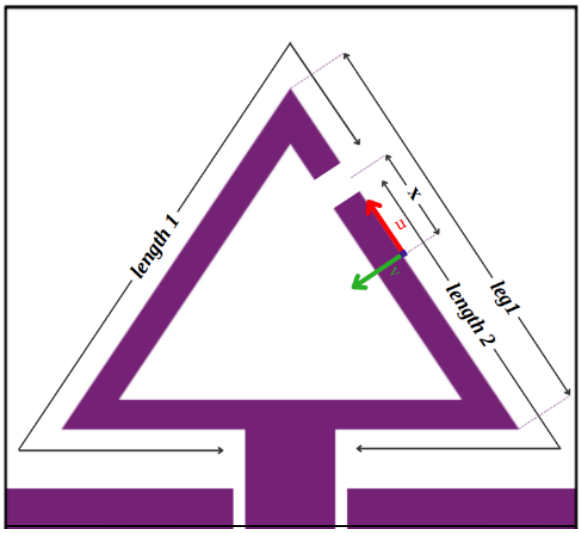

Figure 2.8 Illustration of the slot's position variable x and the two main electrical lengths

The effect of moving the slot on triangle's *leg1* b can be further investigated with the help of parametric study of its position *x*. The reference taken for this *x* is the center of *leg1*, that is illustrated in the schematic of Figure 2.8.

Figure 2.9 provides a clear illustration of how the position of the slot significantly affects both bands of the antenna. Notably, the impact of increasing or decreasing the position of the slot is opposite for the two bands.

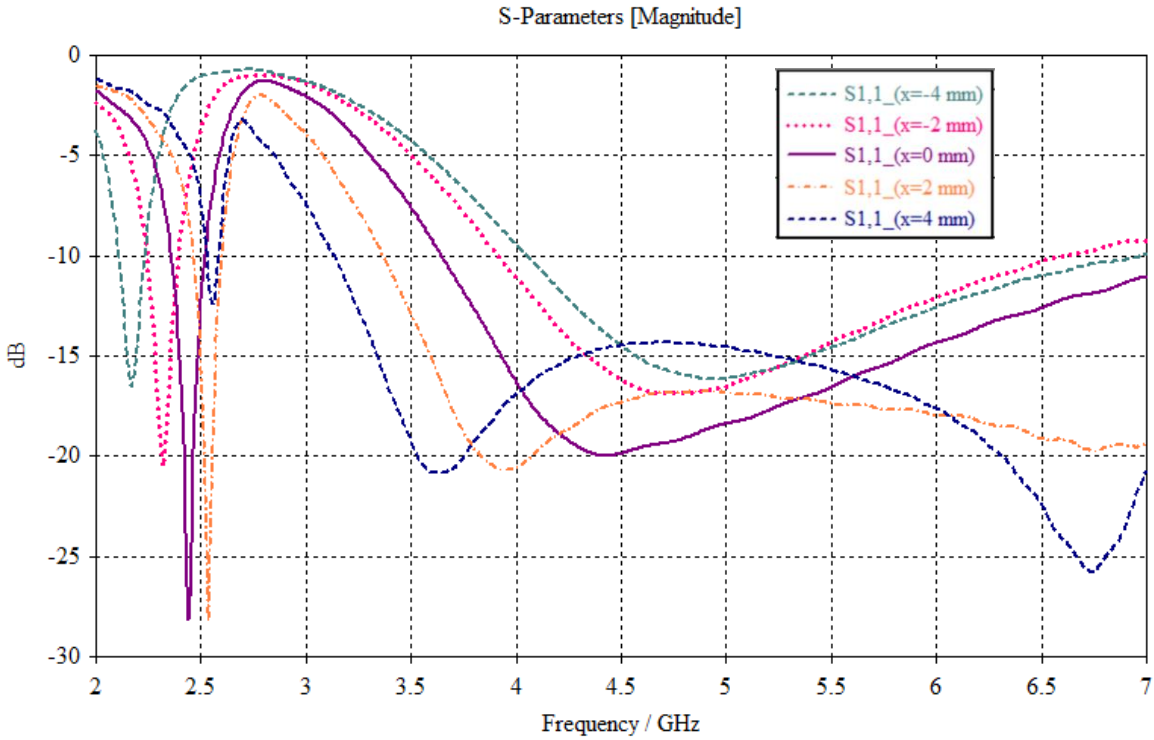

Figure 2.9 The effect of varying the position of the slot on the input reflection coefficient

It can be noticed that we may distinct two main electrical, referred to as *length 1* and *length 2*, as shown in Figure 2.6. These lengths play a crucial role in determining the behavior of the antenna. When *length 1* increases, the first band is shifted towards lower frequencies, while the second band is shifted towards higher frequencies. Conversely, when *length 2* increases, the first band shifts towards higher frequencies, while the second band shifts towards lower frequencies. An important observation can be drawn from these findings: *length 1* primarily influences lower frequencies, while *length 2* predominantly affects higher frequencies.

These results highlight the significance of the slot's position and the electrical lengths in shaping the operational frequency bands of the antenna. Understanding these relationships is necessaire for optimizing the antenna design and achieving the desired frequency

performance. From the different S11 plots it is evident that the optimal position for achieving both desired operating bands with precise resonant frequencies is when the initial position, *x=0*, is utilized.

2.2.4 Current distribution

The way the current is spread across the antenna's surface is important because it shows how the current moves through the antenna after it is fed. This information helps us understand the radiation pattern. In Figure, we can see the simulated current distribution of the CPW antenna at two different frequencies: *2.44GHz* and *4.44GHz*. Interestingly, there are more points of maximum current at the lower frequency compared to the higher frequency. At lower frequencies, the current is mainly concentrated on the feed line and one part of the triangular ring, while at higher frequencies, it is mostly focused on the feed line. These observations confirmed what we have been noticed before about the responsibility of the electrical lengths for both bands.

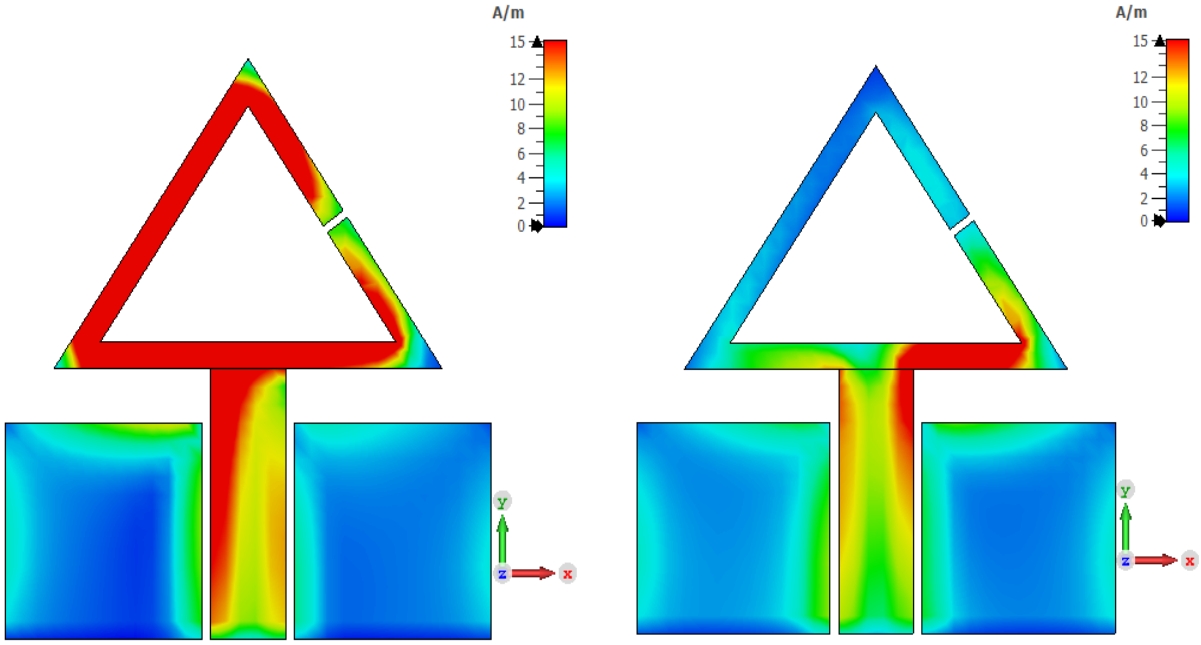

(a) (b)

Figure 2.10 The current distribution at a)2.44Ghz b)4.44Ghz

2.2.5 The 2D Radiation Patterns

The figures below show how the antenna emits its signal in the far field at frequencies of *2.44GHz* and *4.44GHz* in the E-plane (φ=90°) and the H-plane (φ=0°).

At *2.44GHz*, the antenna exhibits dipole like shape radiation in the E-plane with a realized gain of *-1.10dBi* and *0.505dBi*, respectively. In the H-plane, it displays an omnidirectional radiation pattern with a realized gain of *-1.280dBi* and *0.118dBi*, respectively.

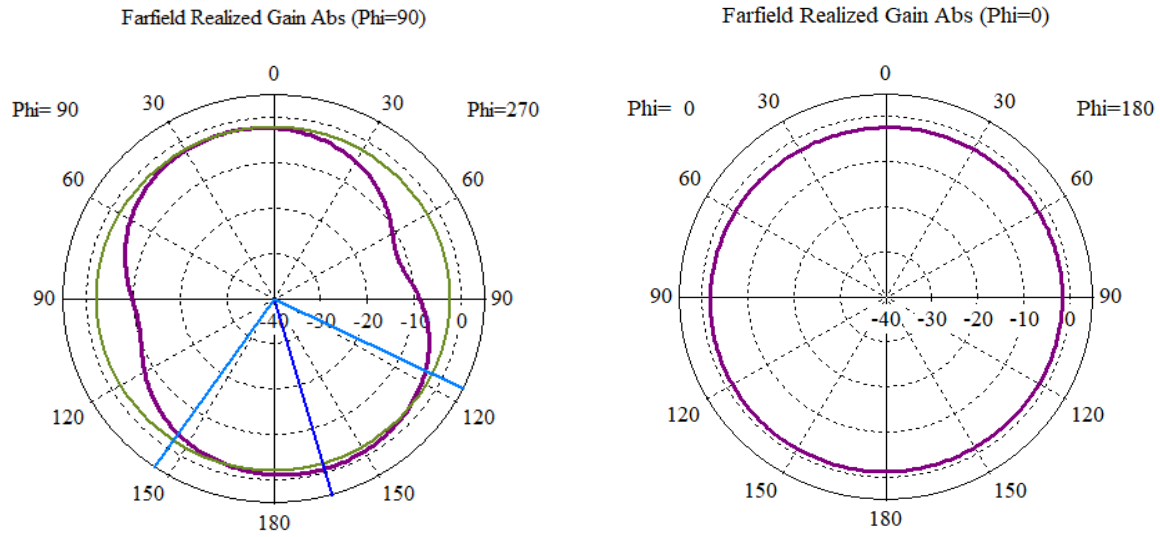

(a) (b)

Figure 2.11 The 2D radiation patterns at 2.44Ghz a) E-plane b) H-plane

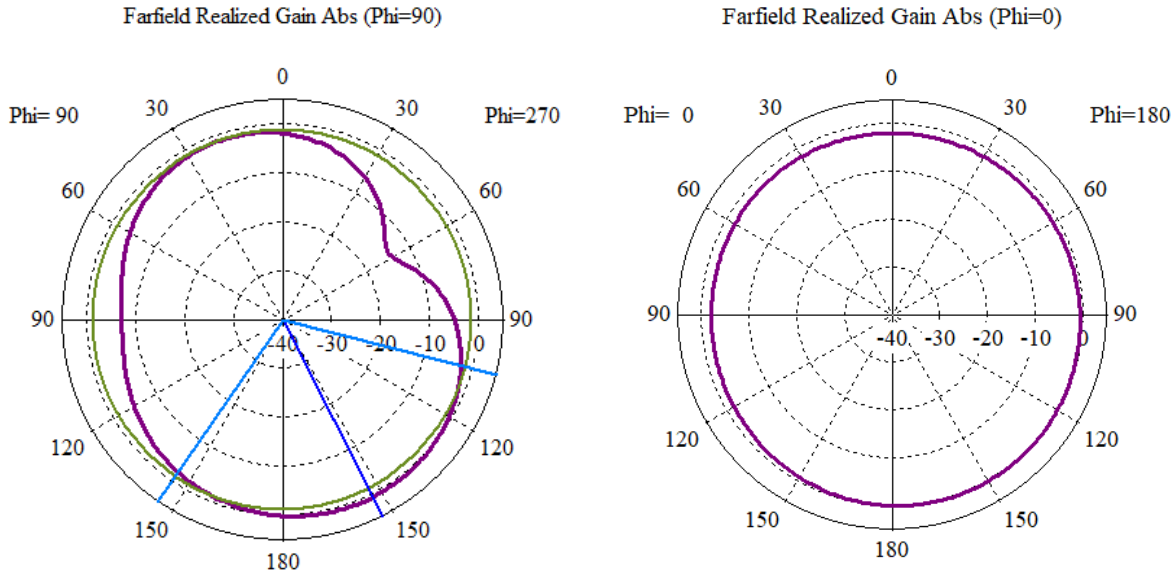

(a) (b)

Figure 2.12 The 2D radiation patterns at 4.44Ghz a) E-plane b)H-plane

2.2.6 The 3D Radiation Patterns

Figure 2.11 shows the simulated 3D radiation patterns of the CPW antenna at *2.44GHz* and *4.44GHz*. At the low resonant frequency, the antenna exhibits an Omni-directional radiation patterns with a peak gain of *2.11dBi*. While at high resonant frequency the antenna exhibit radiation patterns that look like a doughnut with maximum gain of *2.66dBi*.

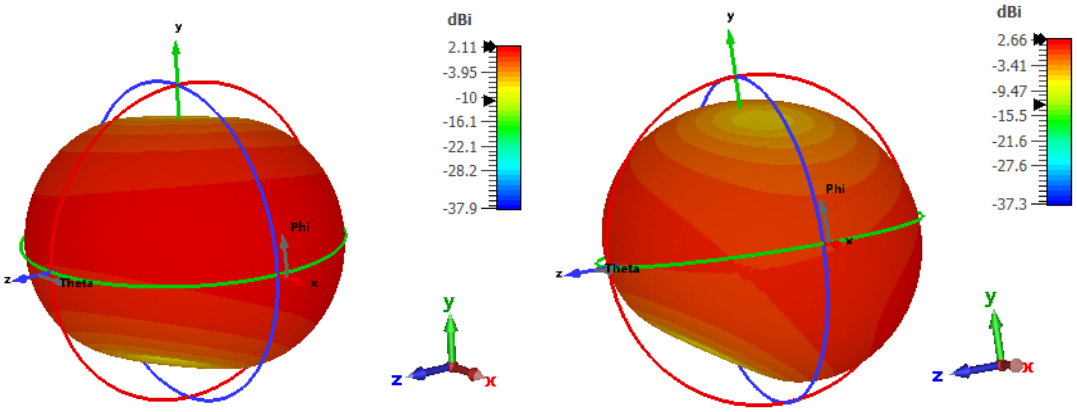

Figure 2.13 The 3D Radiation patterns at a) 2.44GHz b) 4.44GHz

2.3 Conclusion

In this chapter a CPW dual band slotted triangular ring antenna is designed in the aim of covering the WLAN operating bands. The stepwise procedure as well as parametric studies for the most important parameters have been done in order to achieve the optimum design.

In the next chapter we will introduce another ring to benefit from metamaterials characteristics and ,get better results.

Chapter Three
Metamaterial Inspired Dual Band Antenna Design and Analysis

Metamaterial Inspired Dual Band Antenna Design and Analysis

3.1 Introduction

This chapter focuses on the design and analysis of a dual-band compact-sized antenna inspired by the triangular double split-ring resonator DSRR metamaterial. The use of metamaterials is employed to improve antenna characteristics, including size reduction, while maintaining efficient operation.

The chapter is divided into two main parts. The first part focuses on enhancing the antenna design by introducing an inner triangular slotted ring, building upon the findings of the previous chapter. This modification aims to give metamaterial characteristics, so improving the antenna's performance and achieving enhanced dual-band operation. While in the second section of the chapter, the focus shifts towards utilizing the metamaterial's size reduction property to minimize the antenna's physical dimensions while maintaining its dual-band capabilities. This becomes particularly advantageous when operating at low frequencies.

The final proposed antenna is specifically designed to provide coverage for the [*2.38–2.52GHz*] and [*4.24–8.1GHz*] bands, effectively covering the WLAN frequency ranges.

3.2 Inspired Metamaterial Triangular Double SRR Antenna

This part focuses on the integration of a split ring into the existing Antenna III design from Chapter Two, resulting in a triangular double split-ring resonator SRR. While previous studies have primarily explored circular or square geometries, the use of a triangular geometry is comparatively rare [21]. By incorporating this geometry, the antenna's characteristics and performance can be further enhanced. Steps, modifications as well as corresponding results will be presented.

3.2.1 Insertion of Inner Ring

The design and dimensions used in Chapter Two (Figure 2.1, Table 2.1) are kept the same. The gap between the two rings has been taken as *gap=1 mm*. The strong effect of this gap will be discussed in the next part. while the width of the inner ring is the same as the outer one *t=1mm*.

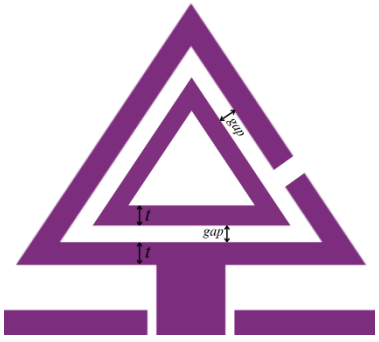

Figure 3.1 Inner Ring Insertion

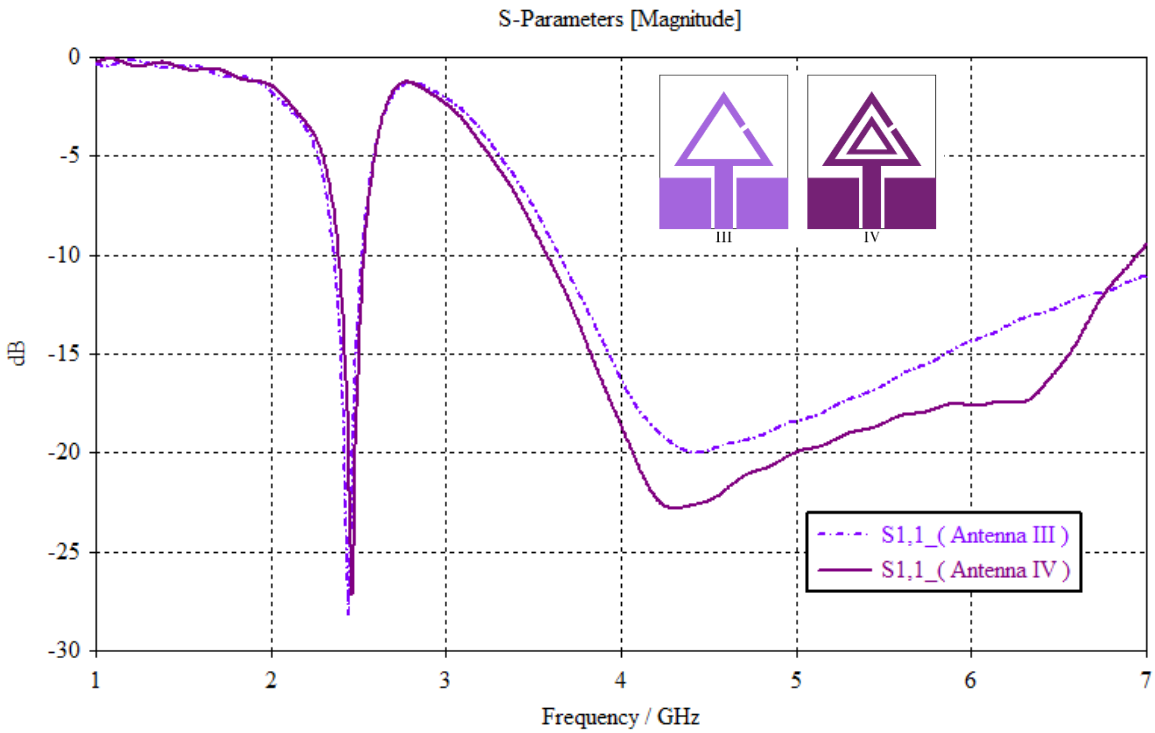

Figure 3.2 The effect of adding the Inner Ring on S11

Figure 3.2 demonstrates the impact of adding the inner ring with a 1mm gap between the rings. Observing the results, it can be concluded that the presence of the inner ring has minimal effect on the antenna's performance. The first operating band remains largely unchanged, while a slight enhancement in matching is observed in the second band, with a reduction in return loss reaching *-22.8dB*. Additionally, a shift towards lower frequencies is observed for the second resonance. These findings indicate that the addition of the inner ring has limited influence on the antenna's characteristics. However, further improvements are expected when the slot is introduced in the subsequent part of the study.

3.2.2 Introducing the Inner Split

To achieve the final configuration of the Split Ring Resonator SRR structure, a split was introduced in the leg of the inner ring. This slot has the same dimensions as the one in the outer ring ‘ width *ts* and length t ’ and was precisely placed in the region opposite to its location ‘leg1’, specifically referred to as *inner leg 2*. The precise position of the slot is denoted as *y* and is visually depicted in Figure 3.3.

The primary objective behind this modification is to further adjust the resonant behavior and enhance the overall performance of the antenna.

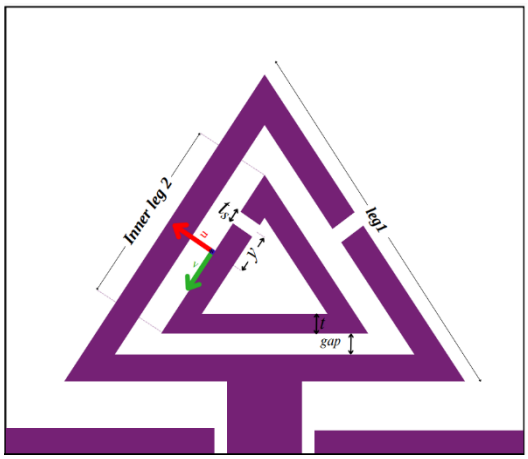

Figure 3.3 Illustration of the inner slot's position variable y

a. Effect of the gap between the two rings

The gap between the rings in the DSRR antenna is a parameter that exerts a significant impact on its performance. Figure 3.4, displaying the input reflection coefficient, demonstrates the influence of the gap size between the two resonators on both operating bands.

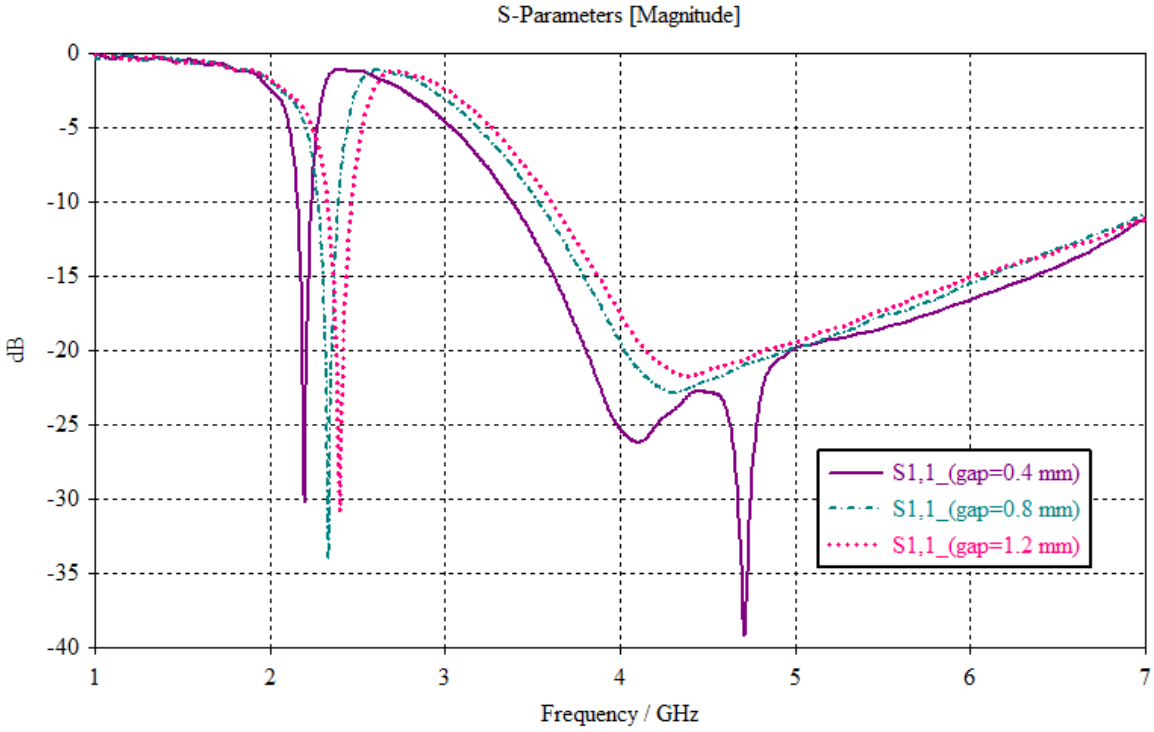

Figure 3.4 Effect of the gap between the two rings on the S11

When the gap is reduced, noticeable changes occur in the antenna's resonant behavior. The first resonance shifts towards lower frequencies as well as the second one, and better matching is achieving. Furthermore, it can be noticed that the width of the gap has an impact

on the antenna's bandwidth. A wider gap results in a broader bandwidth, while a narrower gap yields a narrower bandwidth.

b. Effect of the Inner Slot's position *y*

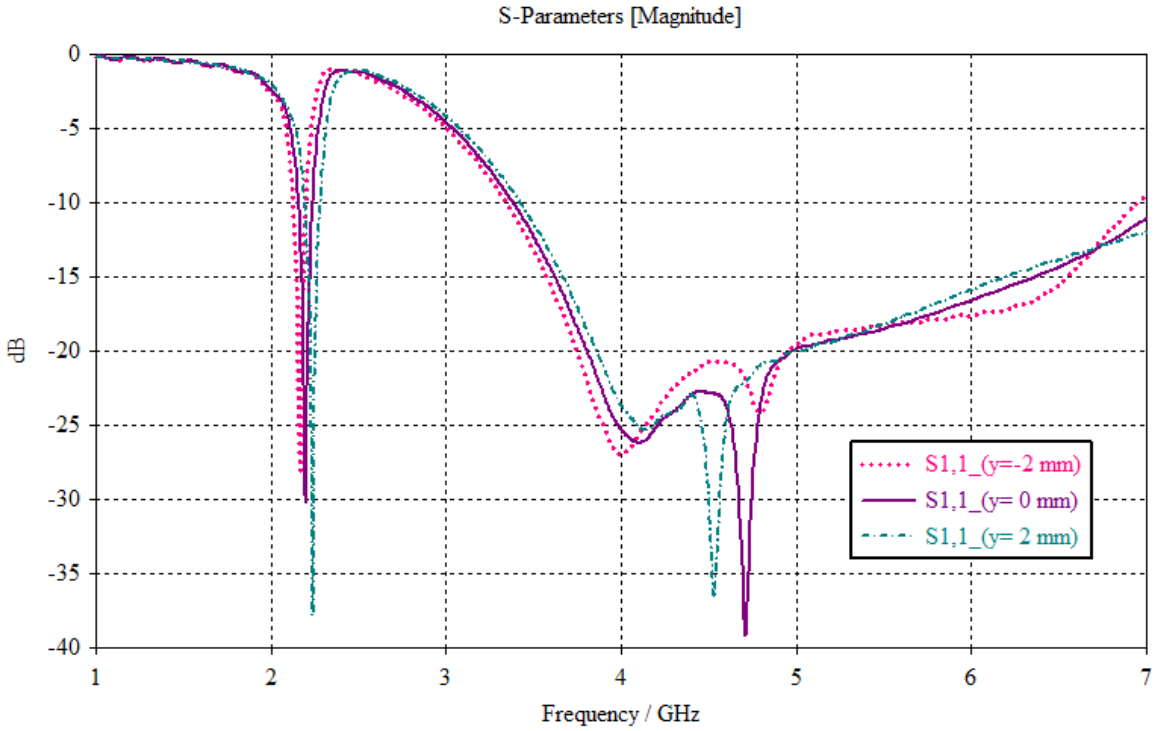

Figure 3.5 The effect of the position of the inner slot on the S11

The insertion of the inner slot on leg 2 of the triangle structure (refer to Figure 3.3) has a noticeable impact on the antenna's characteristics, specifically in relation to the matching of the second band. When the slot is positioned further away from the triangle base, the matching performance shows improvement. However, as the slot moves away from the middle of leg 2 (position *y=0*), there is a slight decrease in matching. Notably, there is a significant resonance shift towards lower frequencies in the same band, while a minor shift towards higher frequencies is observed in the first band, accompanied by improved matching. This behavior highlights the sensitivity of the antenna's performance to the placement of the inner slot and emphasizes the importance of carefully selecting the position to achieve desired performance characteristics.

Based on the obtained results, the antenna demonstrated its ability to operate at a low frequency of 2.15 GHz, which is even lower than the desired lower band. This finding suggests the potential for size reduction of the antenna. The next part of the discussion will

focus on the design and the necessary parametric studies conducted to optimize the antenna's performance and achieve the best results in terms of size reduction.

3.3 Reduced Triangular Double SRR Antenna

Miniaturization of antennas is a crucial aspect in modern wireless communication systems, as it allows for more compact and portable devices with improved performance. The DSSR antenna, inspired by metamaterial structures, offers dual-band operation and has shown promising results in terms of its performance. The miniaturization process involves parametric studies and optimizations to ensure the best performance in terms of impedance matching and bandwidth.

The Figure 3.6 illustrates the geometry and new dimensions of the miniaturized antenna. This representation visually showcases the modified design that has been optimized for size reduction while maintaining its essential characteristics and performance. The overall antenna size has been reduced from $20mm \times 24mm$ *to* $18mm \times 20mm$. As before, it is designed using an FR-4 dielectric substrate with relative dielectric permittivity $\varepsilon_r = 4.3$, loss tangent $tan\delta = 0.025$ and thickness h=1.6mm. Table 3.1 shows the final dimensions for the proposed antenna.

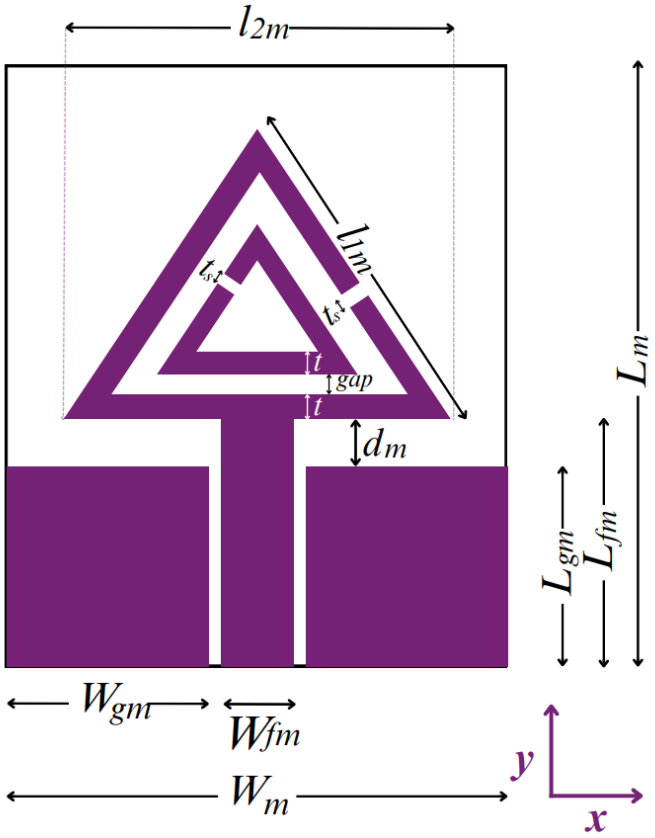

Figure 3.6 Front view of the geometry of the proposed minimized dual band antenna

Table 3.1 The Dimensions of the Proposed Miniaturized Dual-band Antenna

Parameter	L_m	W_m	L_{fm}	Wf_m	Lg_m	Wg_m	$l1_m$	$l2_m$	d_m	t	ts	gap
Value (*mm*)	20	18	8	3.1	6.5	6.08	14	13	1.5	0.8	0.4	0.8

3.3.1 Parametric Study of the Dual band Antenna

To visualize the effect of different parameters on the antenna performance, a parametric study is done by changing one parameter at a time while keeping the remaining constant.

a. Effect of the distance *d* between the ground and the outer Triangle

The simulated reflection coefficient, as depicted in Figure 3.7, showcases the impact of varying the distance *d* in the range of 0.5 to 1.5*mm*. This parameter exhibits a significant influence on the behavior of the second band, while the first band remains largely unaffected. A smaller value of d, *d=0.5mm*, completely eliminates the functionality of the second band. However, as the distance increases, the second band gradually emerges and becomes wider in terms of frequency coverage. Notably, a value of d=1.5*mm* yields excellent results in terms of matching and bandwidth, making it an optimal choice to achieve both compact size and desirable performance.

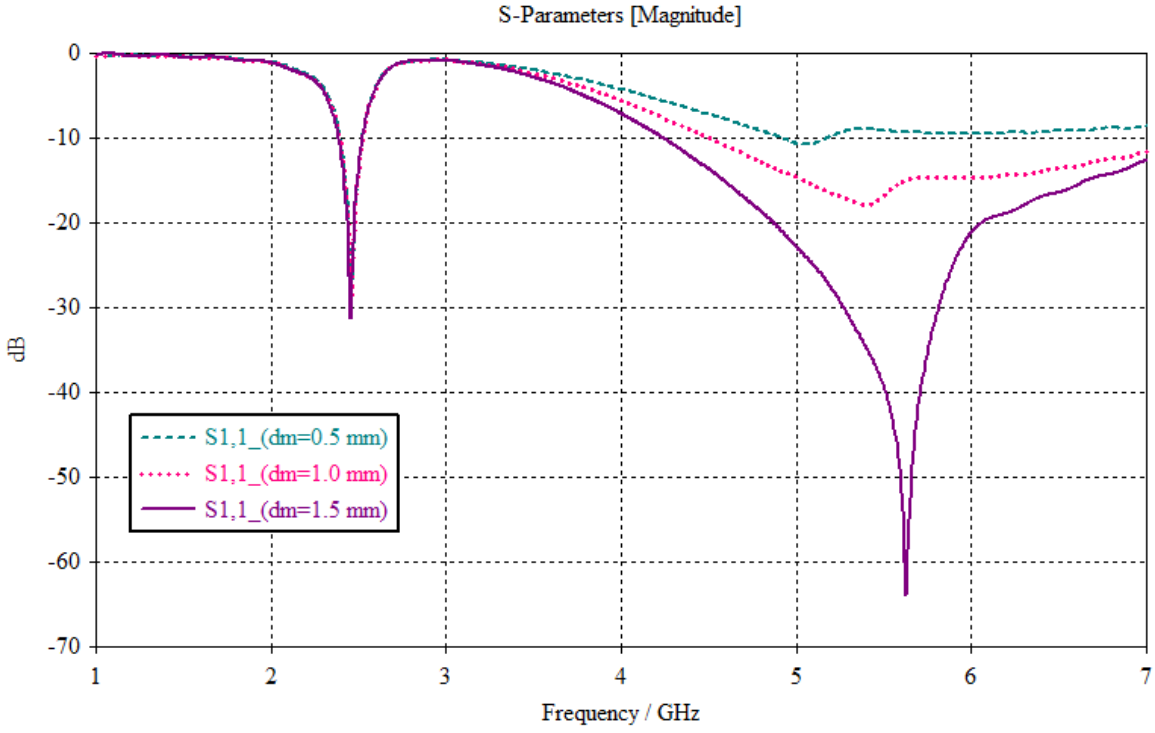

Figure 3.7 Effect of the distance d between the ground and the outer Triangle on the S11

b. Effect of varying the gap between the resonators

The effect of distance variation in DSRR structures has been previously explored. However, the addition of the second split introduces significant changes to the antenna's performance. Therefore, it is necessary to reexamine this parameter for better understanding, as it plays a crucial role in DSRR structures.

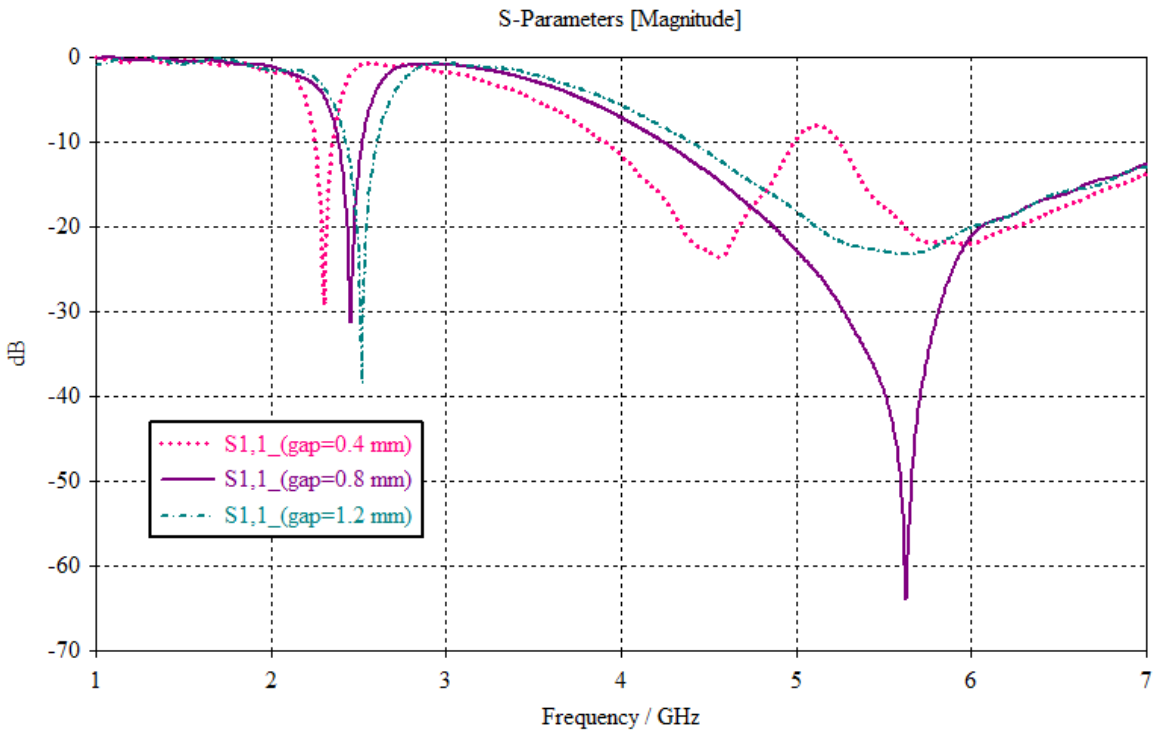

Figure 3.8 The effect of varying the gap between the two rings

As the gap between the resonators decreases, both bands exhibit a closer proximity to each other. Noticeably, there is a significant shift towards lower frequencies observed in the first band. In terms of the second band, the changes are evident in the bandwidth and matching characteristics. For *gap=0.4mm*, the second band experiences a shift to the frequency range of *3.9GHz* to *5GHz*, while a third band emerges at *5.25GHz*. Additionally, it is worth mentioning that a favorable matching and wide bandwidth are achieved with a gap of 0. *mm*, making it an optimal value for our requirements.

c. Effect of varying the width *t* of the rings

The width parameter *t* plays a crucial role in determining the performance of the antenna and it is taken to be the same for both inner and outer rings. Figure 3.9 presents the S11 results, highlighting the significant influence of this parameter on two frequency ranges. In the lower frequency range, an increase in the width leads to a shift towards higher

frequencies, accompanied by noticeable improvements in matching. In the second frequency range, an observation of a triple band functionality is made for *t=0.4mm*, while sacrificing the wide bandwidth in the second range. After careful consideration, an optimum value of *t=0.8mm* is chosen, as it provides a wide bandwidth for the second band and meets the desired design specifications.

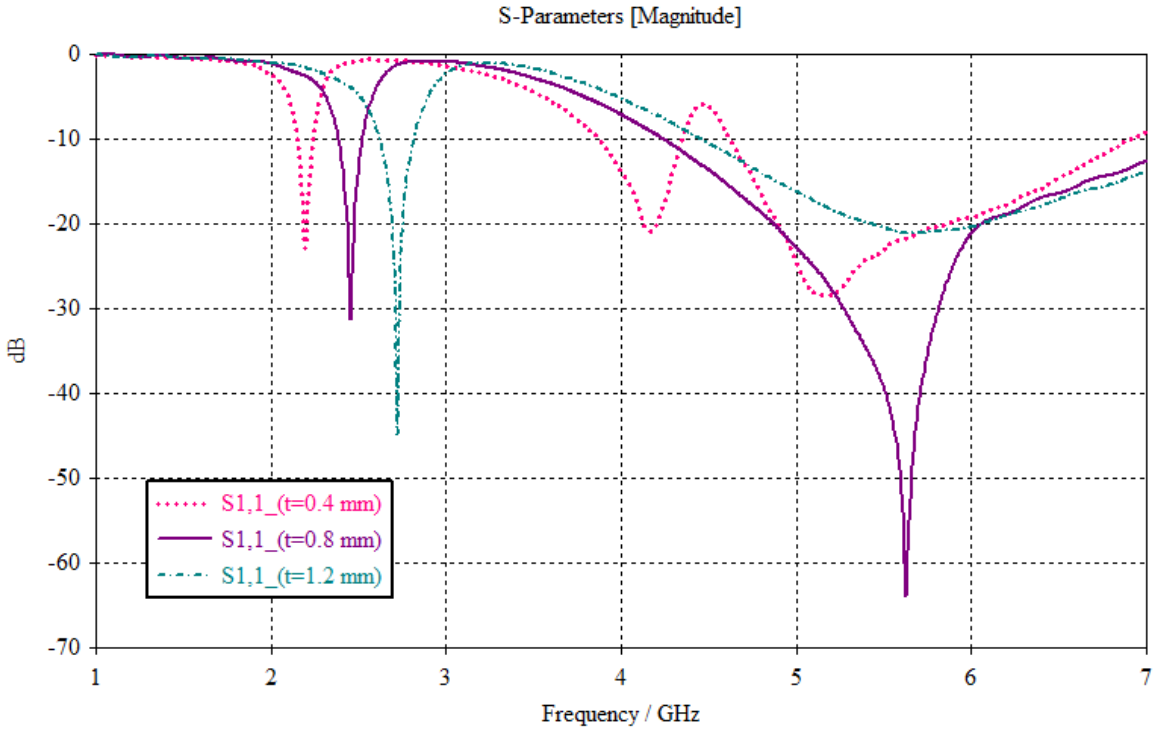

Figure 3.9- The effect of changing the width of the rings t on S11

The effect of varying the position x of the outer split

The transition of the antenna structure from a single SRR to a DSRR configuration necessitates an examination of the outer split position. Figure 3.10 illustrates the S11 results, revealing the effects of varying the position *x* on multiple aspects: operating bands and their resonances, matching, and bandwidth.

In the first band, a consistent trend is observed as the slot position moves from the base towards the top edge of the ring: a shift towards higher frequencies accompanied by a degradation in matching. On the other hand, this position variation forces the second band to move towards lower frequencies, resulting in non-uniform changes in their respective bandwidths. A notable value that yields interesting results is *x = -1.4mm.*

-

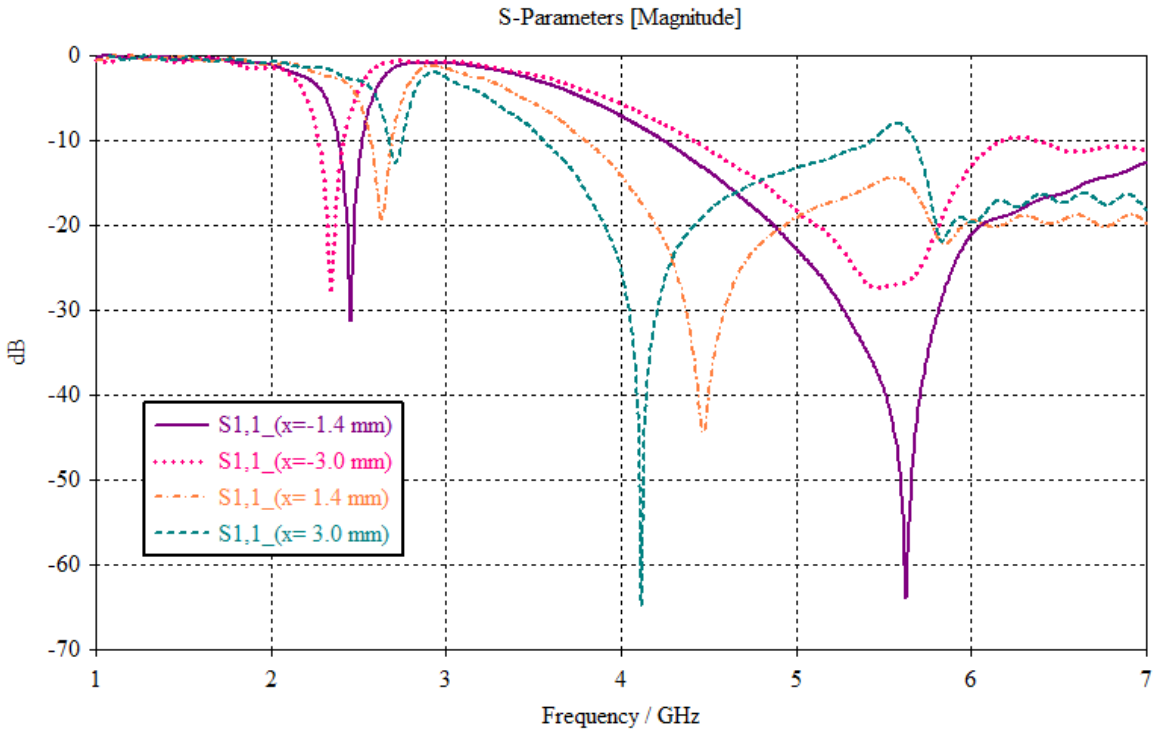

Figure 3.10 Effect of varying the outer split position x

d. Effect of varying the position y of the inner split

In order to investigate the impact of changing the position of the inner slot on the input reflection coefficient, a parametric study was done; involving the analysis of the effect of varying its position while keeping the position of the first slot fixed at *x=-1.4mm.*

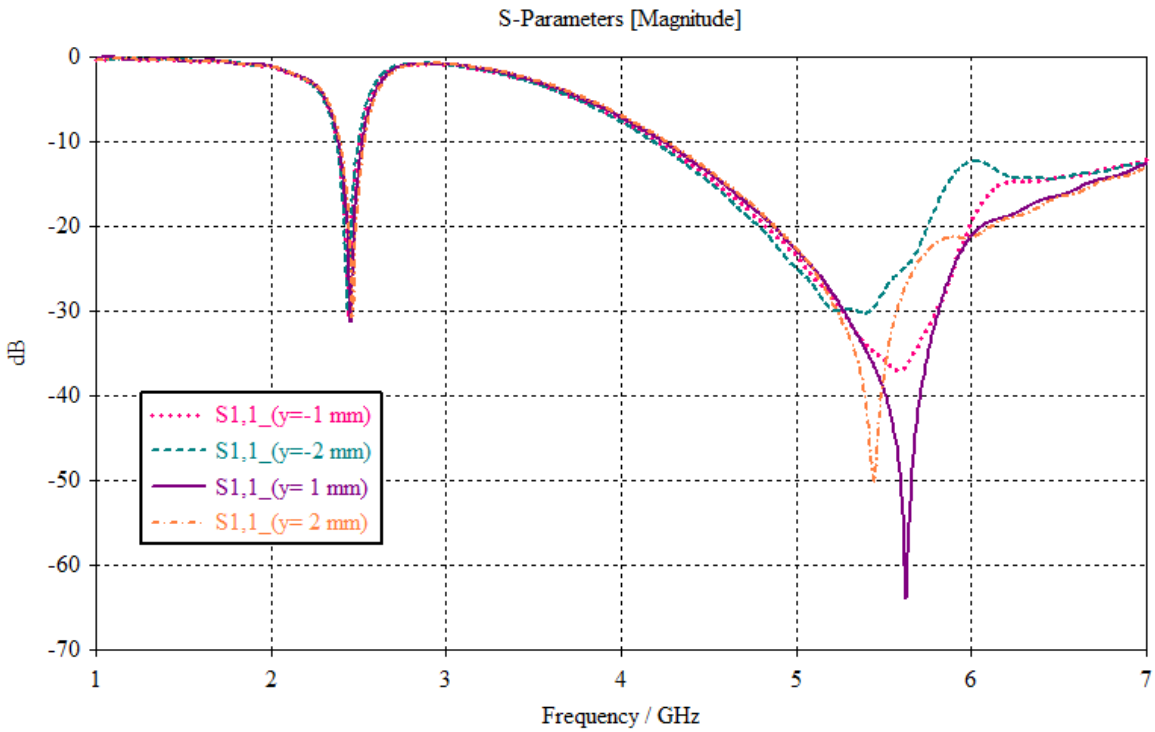

Figure 3.11 The effect of varying the inner split position y

It is evident that the position of the inner slot primarily affects the frequencies in the second band in terms of matching and frequency resonance, while it does not have a big effect on the first band.

When considering negative values of *y*, a noticeable shift in frequencies towards lower frequencies can be observed, accompanied by a decrease in matching performance. Similarly, positive values of *y* exhibit a shift towards lower frequencies and a decrease in matching quality. For design requirements, it was appropriate to choose the position *y=1* for the inner slot.

3.3.2 The current distribution

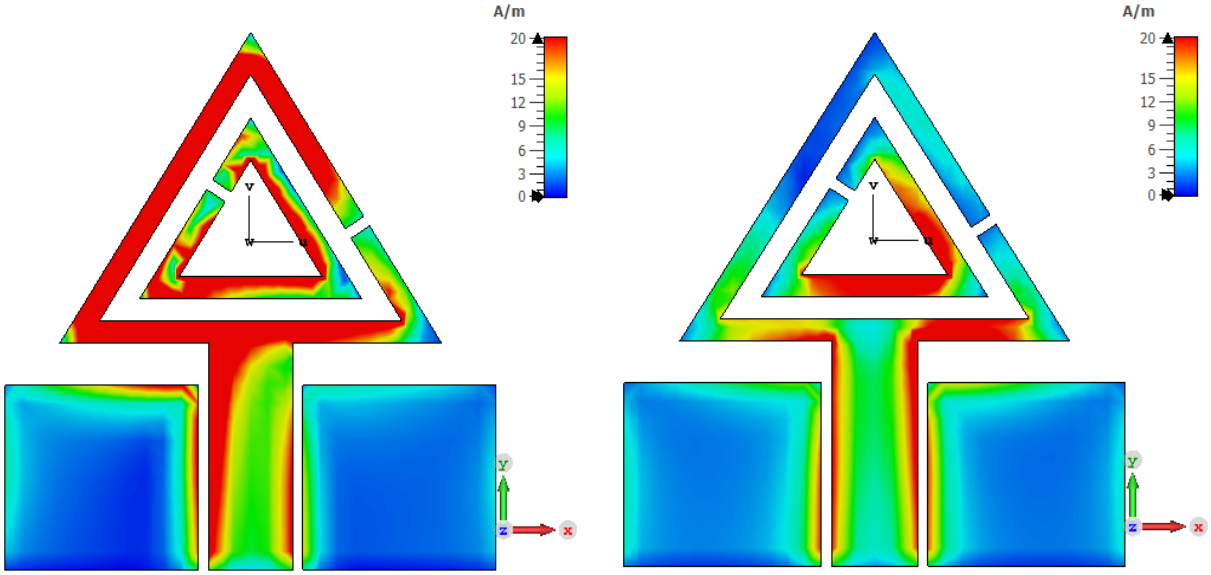

(a) (b)

Figure 3.12 The current distribution at a)2.452Ghz b)5.626Ghz

Figure 3-20 displays the simulated current distributions for the proposed inspired metamaterial dual-band antenna operating at the resonance frequencies of *2.452GHz* and *5.626GHz*.

At *2.452GHz*, the surface current primarily concentrated along the first electrical length resulted by the outer split, resembling the behavior of a single ring antenna. Additionally, it is noteworthy that nearly the entire inner ring emits radiation.

When operating at *5.626GHz*, the surface current distribution remains focused on the base of the inner ring base and the its non-slotted leg, while no current flows through the slotted one. Simultaneously, the current is also distributed along the second electrical length of the outer ring.

3.3.3 The Radiation Patterns

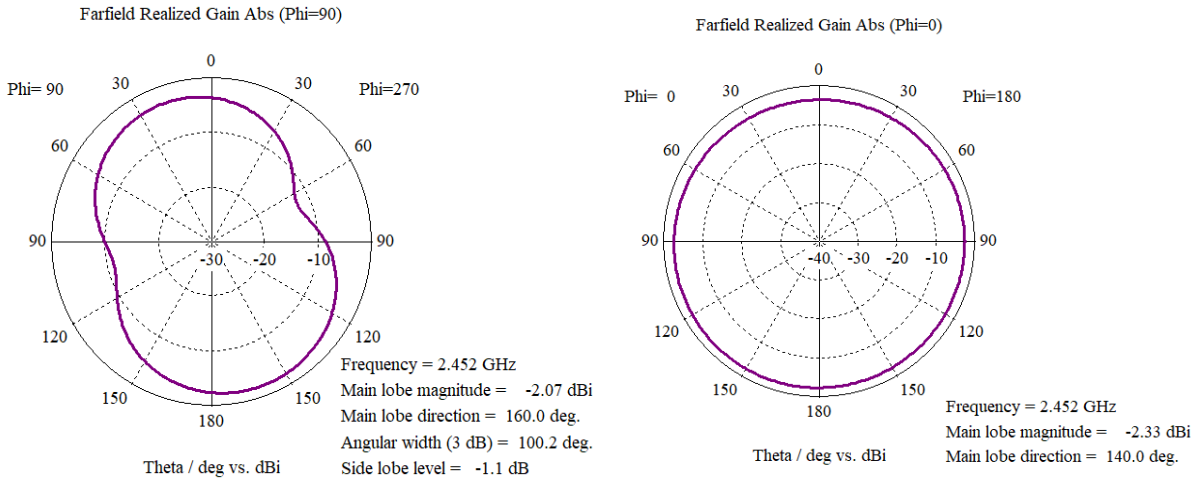

(a) (b)

Figure 3.13 The 2D radiation patterns at 2.452Ghz a) E-plane b) H-plane

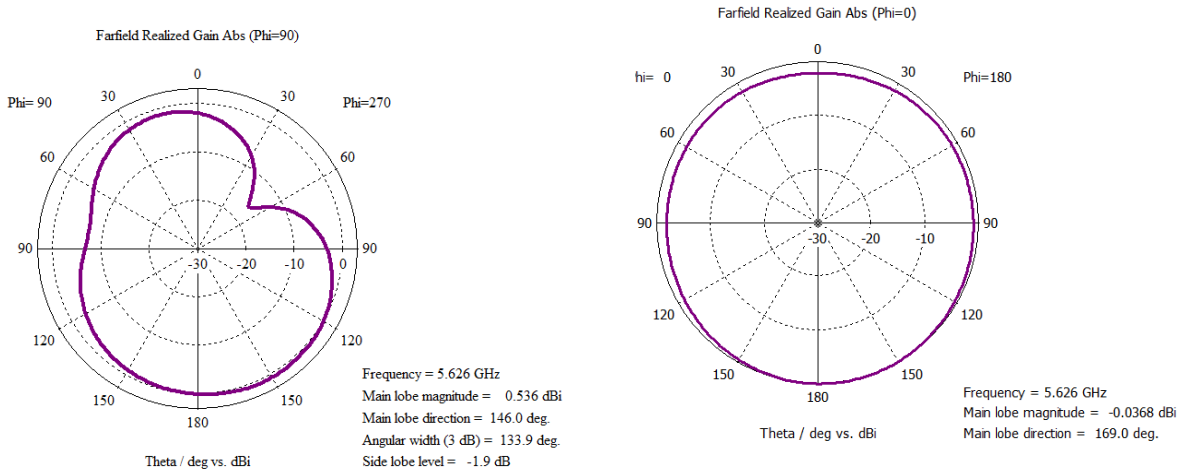

(a) (b)

Figure 3.14 The 2D radiation patterns at 5.626Ghz a) E-plane b) H-plane

Figure 3.12 and Figure 3.13 depict the simulated E-plane and H-plane radiation patterns of the proposed antenna at the two resonant frequencies *2.452GHz* and *5.626GHz*, respectively. The observed patterns exhibit monopole-like radiation characteristics in the E-plane, while displaying omni-directional radiation properties in the H-plane.

Figure 2.15 shows the simulated 3D radiation patterns of the antenna at the resonant frequencies. The radiation pattern looks like a doughnut, similar to a dipole pattern at the lower band resonant frequency. While at the higher band resonant frequency, the pattern looks like a slightly pinched doughnut.

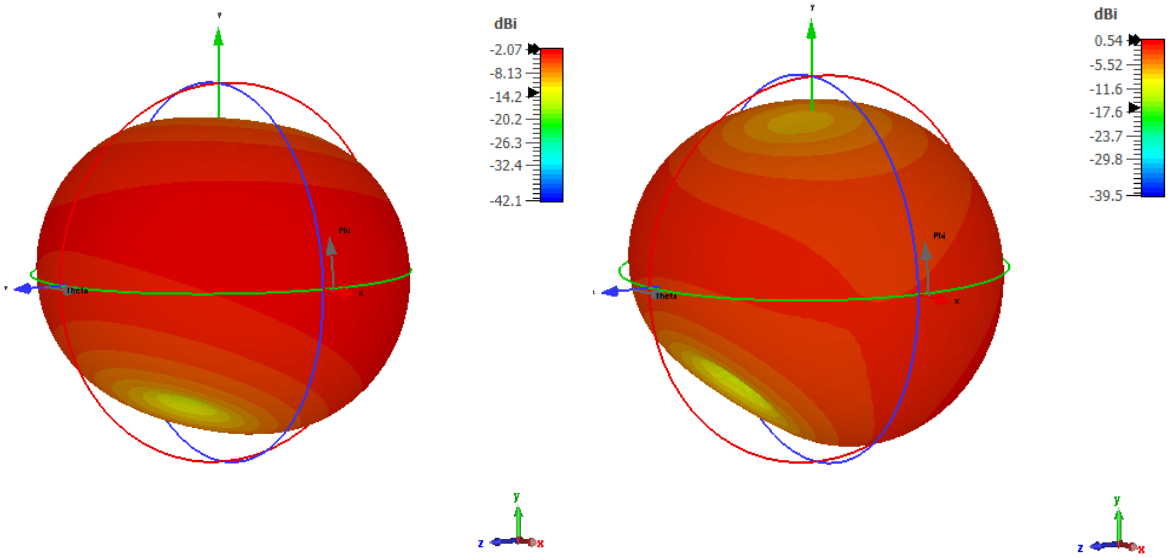

(a) (b)

Figure 3.15 The 3D radiation patterns at a) 2.452GHz b)5.626GHz

3.4 Realization and Measurement of the Miniaturized Metamaterial Inspired Dual Band Antenna

Once the simulated design is thoroughly analyzed and studied using the CST software, the next step involves fabricating the structure. By fabricating the antenna, the obtained results can be compared with the simulated design results.

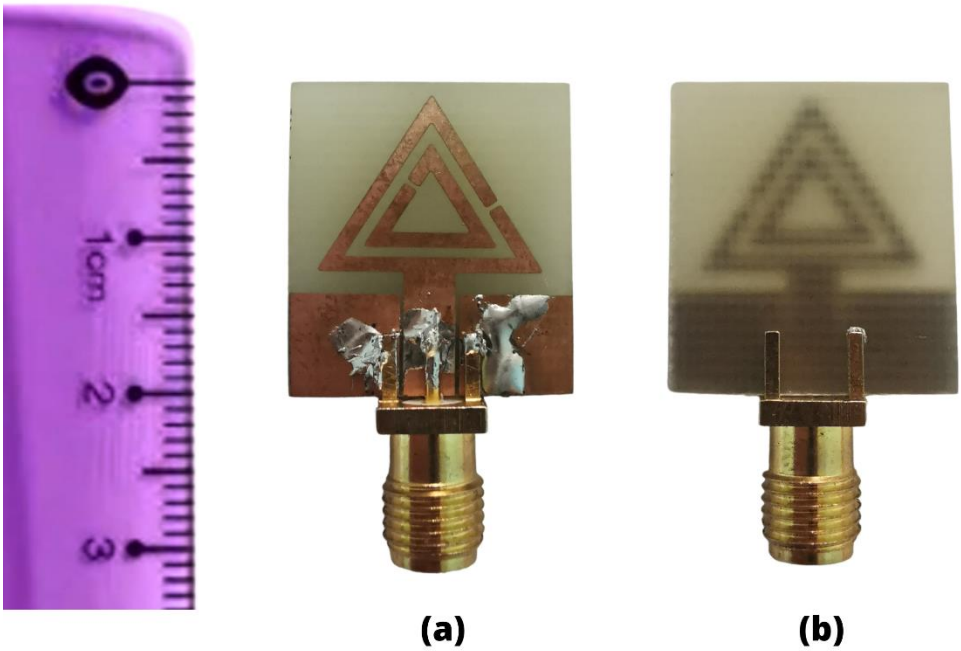

Figure 3.16 Photograph of the realized Metamaterial Inspired Dual Band Antenna a)Front view b)Back view

The input reflection coefficient of the fabricated antenna has been measured using the vector network analyzer VNA. the measurements were carried out at telecommunication INELEC laboratory.

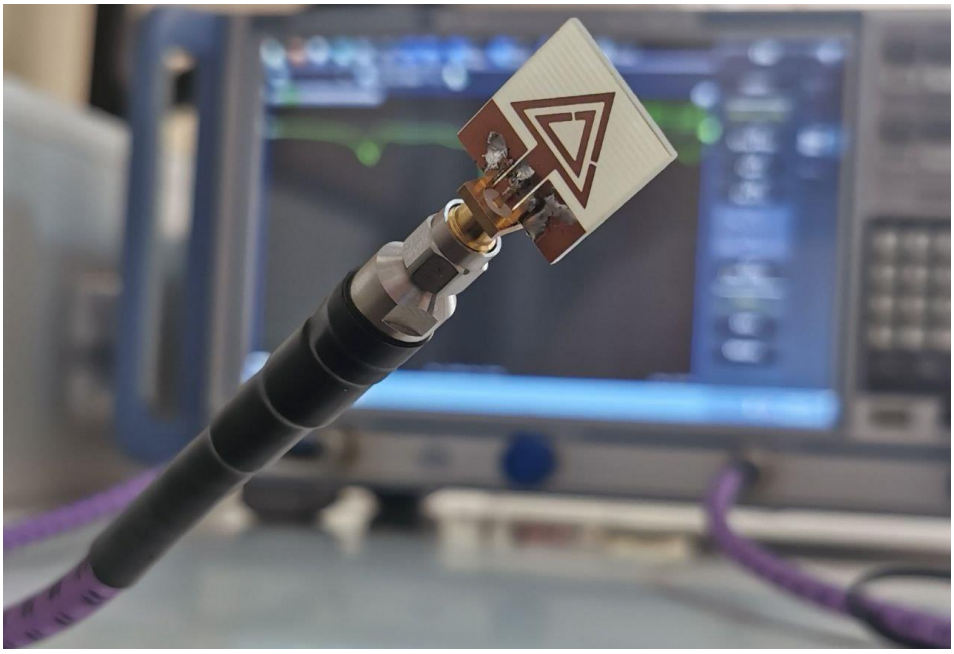

Figure 3.17 Antenna measurements configuration

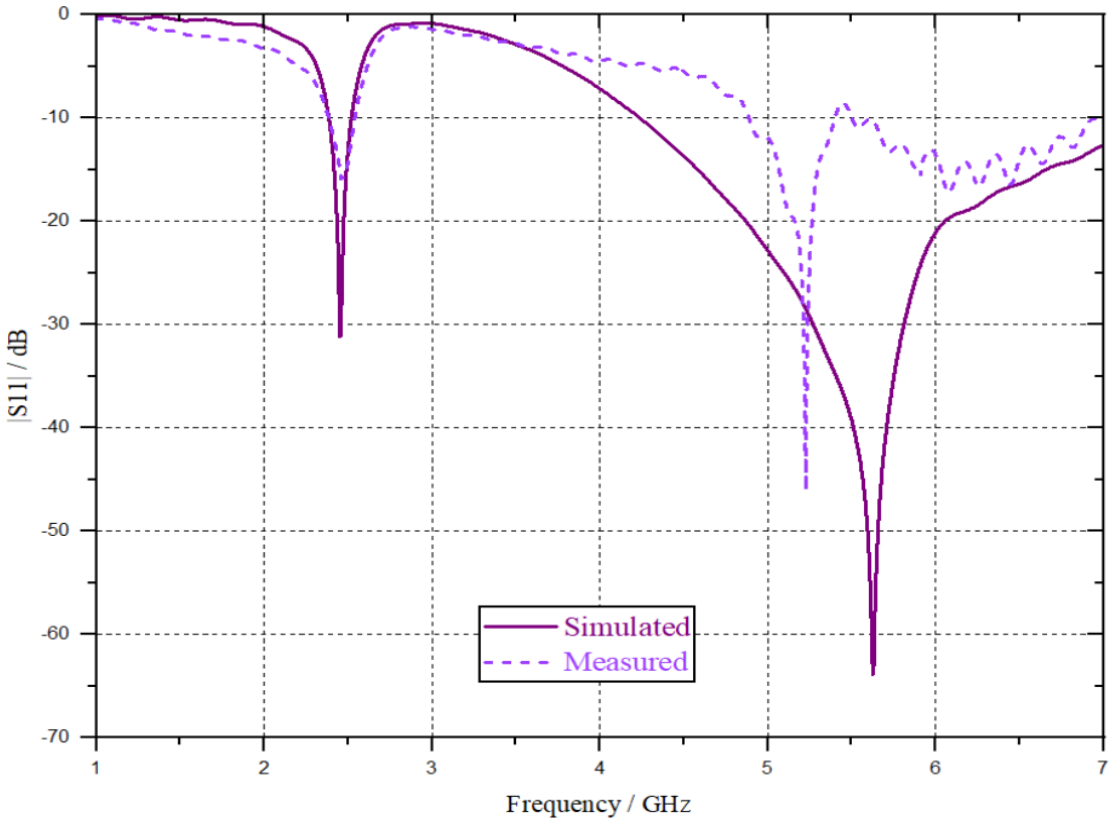

Figure 3.18 Simulated vs Measured input reflection coefficient

Figure 3.18 illustrate the simulated results, and measured input reflection coefficient S11.

While there is a strong overall agreement between the simulated and measured results, except for the second band which is not wide, certain factors contribute to this discrepancy. The manufacturing process, the small antenna size and their parameter sensitivity (e.g., slot positions and widths), material characteristics, and measurement environment which include reflecting obstacles, and the substrate dielectric constant variations, can explain these differences.

3.5 Comparison with Related Works

To see how well the proposed dual band antenna is, a comparison is made with other related works and summarized in Table 3.2.

Table 3.2 Comparison with related works

	Size mm^3	*Operating bands* *GHz*	*S11* *dB*	*Bandwidth* *Percentage %*
[25]	*60 × 50 × 1.6*	*[2.3 - 2.53] 2.45* *[5.05 -6.31] 5.3*	*-18.3* *-23.2*	*9.38* *23.7*
[26]	*20 × 40 × 1.6*	*[2.37 - 2.41] 2.4* *[5.72 - 5.88] 5.8*	*-16.1* *-12.1*	*1.66* *2.2*
[24]	*20 × 24 × 1.6*	*[2.4 - 2.48] 2.45* *[4.7 - 6.04] 5.45*	*-27* *-36*	*1.63* *24.58*
proposed	*18 × 20 × 1.6*	*[2.38 - 2.52] 2.45* *[4.24 – 8.1] 5.62*	*-31.20* *-63.90*	*5.71* *68.68*

As can be concluded from the table , the proposed antenna gives much better results comparing to other antennas in term of the covered operating bands, it also gives the largest percentage bandwidth with the best values of the magnitude of S11 with the smallest size.

3.6 Conclusion

In this Chapter, minimized metamaterial inspired dual band antenna that is suitable for WLAN applications at *2.45GHz* and *5.62GHz* has been proposed.

Input reflection coefficients and far-field properties of the antenna are simulated. The antenna is then fabricated and good result agreement between simulation and measurement is achieved. Furthermore, a comparison with other related works have been done and it highlights the performance of the proposed antenna in terms of size, operating bands, bandwidth, and matching.

General Conclusion

In this project, a miniaturized metamaterial-inspired dual-band antenna utilizing a coplanar waveguide CPW feed has been successfully designed and fabricated to cover the WLAN 2.4GHz and 5.4GHz operation bands. The initial design process began with a triangular patch antenna and evolved into a single triangular slotted antenna, Antenna III, that showed promising results for dual-band functionality.

To further improve the performance of the antenna's second band, an investigation into a double split ring resonator SRR has been conducted. The inclusion of the SRR introduced metamaterial characteristics and effectively shifted the frequency bands towards lower frequencies. Consequently, the proposed antenna achieves a size reduction of 25% as compared to the mono ring slotted triangular antenna, accompanied by a significantly wider bandwidth coverage *[2.38 - 2.52GHz], [4.24 – 8.1GHz]*, with S11of *-31.20dB* and *-63.90dB* at *2.452GHz and 5.626GHz*, respectively. The fabricated antenna has exhibited good agreement between simulated and measured results, confirming its effectiveness.

Finally, a comparison with other related works has been done, where the proposed antenna showcased several favorable attributes, including wide operating bands, broad bandwidth, good impedance matching an overall size of only $18 \times 20 \times 1.6\ mm^3$.

As further work, exploring the enhancement of antenna gain using metamaterials such as Artificial Magnetic Conductor AMC could be of great interest. By incorporating AMC metamaterial, which functions as a reflective surface, the radiated power in specific directions can be amplified. This has the potential to significantly improve antenna performance and extend signal coverage.

References

[1] J. S. Varma and S. K. Dash, "Microstrip-line fed Dual-band L-shaped Antenna with Monopolar Characteristics for Application in WLAN," *IEEE,* 2022.

[2] Y. Huiming , . L. Xinyi and L. Haihong , "Dual-Band Microstrip Antenna Based on Polarization Conversion Metasurface Structure," 2020.

[3] M. Hussain, . A. A. Wahaj and M. Alzaidi, "Metamaterials and Their Application in the Performance Enhancement of Reconfigurable Antennas," *Micromachines (Basel),* 2023.

[4] K. DJAFRI, "Contribution to the Study and Design of Miniaturized Microstrip Antennas," Boumerdes,Algeria, 2018/2019.

[5] V. Paraforou, " Design and full-wave analysis of supershaped patch antennas," Delft, The Netherlands, 2013.

[6] S. Narinder, "A Study Of Different Feeding Mechanisms In Microstrip Patch Antenna," *International Journal of Microwaves Applications*, February 2017.

[7] C. Balanis, Antenna theory: Analysis and design, fourth edition, New York, 2016.

[8] F. GUICHI, "Study and Design of Planar Antennas for UWB," Boumerdes,Algeria, 2018.

[9] D. Gadhavi and T. Pansuriya, "2.45 GHz Antenna Designs with Impedance Matching Network," School of Information Technology,Halmstad University,Sweden, 2018.

[10] A. AZRAR, *"Course Handout of Antennas",* Institute of Electrical and Electronic Engineering, university of Boumerdes, Algeria.

[11] "IEEE Standard Definitions of Terms for Antennas, Transactions on antennas," May

1969.

[12] B. Baumann, "Polarization Sensitive Optical Coherence," *Applied Sciences,* 2017.

[13] K. Fujimoto, Mobile Antenna Systems Handbook, Third Edition, Boston, LONDON, 2008.

[14] Y. Y. WOLDEAMANUEL, "Design of a 2.4 GHz Horizontally Polarized Microstrip Patch Antenna using Rectangular and Circular Directors and Reflectors," The University of Texas , Tyler, 2012.

[15] R. Kumar, M. Kumar, J. S. Chohan and . S. Kumar, "Overview on metamaterial: History, types and applications," *Sciencedirect,* 2022.

[16] D. R. Smith, M. C. K. Wiltshire and . J. B. Pendry, "Metamaterials and Negative Refractive Index," *Science,* Aug. 2004.

[17] J. Canet-Ferrer, Metamaterials and Metasurfaces, London, United Kingdom: IntechOpen, 2019.

[18] K. Gangwar, Dr. Paras and Dr. R.P.S. Gangwar, "Metamaterials: Characteristics, Process and Applications," *ReaserchGate,* January 2014.

[19] F. Mouhouche, "Study and Analysis of Metamaterial," Boumerdes,Algeria, 2018/2019.

[20] W. J. Krzysztofik and N. C. Thanh , Metamaterials in Application to Improve Antenna Parameters, November, 2018.

[21] P. S. Manage, U. Naik, S. Nargundkar and V. Rayar, "A Survey on applications of Metamaterials in Antenna Design," in *Smart Systems and Inventive Technology ICSSIT*, Karnataka-India, 2019.

[22] X. C. Tong, "Functional Metamaterials and Metadevices," *Springer,* 2018.

[23] K. Sarabandi and N. Behdad, "A Frequency Selective Surface With Miniaturized," *IEEE,* May 2017.

[24] G. Priyanka and J. Priyanka , "Design and analysis of a metamaterial inspired dual band antenna for WLAN application," *nternational Journal of Microwave and Wireless Technologies,* 2018.

[25] Tai L-C "A dual-band bow-tie-shaped CPW-fed slot antenna for WLAN applications". *Progress In Electromagnetics Research*

[26] Ali MSM, Rahim SKA, Sabran MI, Abedian M, Eteng A and Islam MT "Dual band miniaturized microstrip slot antenna for WLAN applications". *Microwave and Optical Technology Letters, 2018*

Appendix

CST MICROWAVE STUDIO

CST STUDIO is a powerful simulation platform for all kinds of electromagnetic field problems and related applications. It provides a large package of simulation modules; one of them is CSTMICROWAVE STUDIO.CST MICROWAVE STUDIO CST MWS is a specialist tool for the 3D EM simulation of high frequency components. CST MWS enables the fast and accurate analysis of high frequency HF devices such as antennae, filters, couplers, planar and multi-layer structures and SI and EMC effects. CST software makes available Time Domain and Frequency Domain solvers, CST MWS offers further solver modules for specific applications. Filters for the import of specific CAD files and the extraction of SPICE parameters enhance design possibilities and save time. It is based on the finite integration technique FIT. It allows to choose the time domain as well as the frequency domain approach. The Time Domain Solver calculates the broadband behavior of electromagnetic devices in one simulation run with an arbitrarily fine frequency resolution. The modeling of curved structures using the Perfect Boundary Approximation technique and the modeling of thin perfectly electric conducting sheets with the Thin Sheet Technique tries to cope with the typical difficulties inherent to classical FDTD methods. CST, as a general- purpose software package being a real competitor for HFSS, has gained popularity in the last few years. Also, for the analysis and design of planar and small antennas. A problem in CST is the ripples in the frequency response in case the tool box is not appropriate. This is due to the fact that the flag ship of CST is a time domain solver.